Article (refereed) - postprint

Dumont, Egon; Williams, Richard; Keller, Virginie; Voss, Anja; Tattari, Sirkka. 2012 Modelling indicators of water security, water pollution and aquatic biodiversity in Europe. *Hydrological Sciences Journal*, 57 (7). 1378-1403. 10.1080/02626667.2012.715747

Modelling indicators of water security, water pollution, and aquatic biodiversity in Europe

Egon Dumont[1], Richard Williams[1], Virginie Keller[1], Anja Voß[2], Sirkka Tattari[3]

[1]*Centre for Ecology & Hydrology (CEH), Maclean Building, Benson Lane, Crowmarsh Gifford, OX10 8BB, United Kingdom*
egdu@ceh.ac.uk
[2]*Center for Environmental System Research (CESR) University of Kassel, Kurt-Wolters-Str. 3, D-34125 Kassel, Germany*
[3]*Finnish Environment Institute (SYKE), Mechelininkatu 34a, P.O. Box 140, 00251 Helsinki, Finland*

Abstract The GWAVA (Global Water AVailability Assessment) model for indicating human water security has been extended with a newly developed module for calculating pollutant concentrations. This module is described in this paper. The module is illustrated by using it to model nitrogen, phosphorus and organic matter concentrations. The module solely uses input variables that are likely to be available for future scenarios, making it possible to apply the module to such scenarios. The module first calculates pollutant loading from land to rivers, lakes, and wetlands by considering drivers such as agriculture, industry, and sewage treatment. Calculated loadings are subsequently converted to concentrations by considering aquatic processes such as dilution, downstream transport, evaporation, human water abstraction, and biophysical loss processes. Aquatic biodiversity is indicated to be at risk if modelled pollutant concentrations exceed certain water quality standards. This is indicated to be the case in about 35% of the European area, especially where lakes and wetlands are abundant. Human water security is indicated to be at risk where human water demands cannot be fulfilled during drought events. This is indicated to be the case in about 10% of the European area, especially in Mediterranean, arid, and densely populated areas. Modelled spatial variation in concentrations matches well with existing knowledge, and the temporal variability of concentrations is modelled reasonably well in some river basins. Therefore we conclude that the updated GWAVA can be used for indicating changes in human water security and aquatic biodiversity across Europe.

Key words water resources; eutrophication; modelling; BOD; nitrogen; phosphorus; Europe; GWAVA; water scarcity; water quality; Water Framework Directive

INTRODUCTION

The requirement to manage water resources in an integrated and sustainable manner has become a driving force behind the use of large-scale gridded models (Xu and Singh 2004). Such models have traditionally focused solely on availability of water resources for direct human use. However, the quality of freshwater resources for supporting the diversity of native species is an important aspect (Millennium Ecosystem Assessment 2005), especially because native species can sustain important ecosystem services such as food and recreation (Loomis *et al.* 2000).

Modelling impacts of changing water resources on biodiversity requires consideration of water quality and its variability over large spatial and temporal scales. This large-scale variability is important because global drivers such as population growth and climate change are likely to have widespread and long-term impacts on water quality. Population growth has widespread impacts on water quality due its effects on agricultural and industrial production and waste disposal (Billen *et al.* 2010, Hoekstra 2011). Global climate change impacts may decrease water quality through reduced dilution capacity of some rivers because of more frequent droughts, or increased pollutant loadings to other rivers due to changed rainfall patterns (Bates *et al.* 2008).

Five-day biochemical oxygen demand (BOD_5), total nitrogen (TN) concentration, and total phosphorus (TP) concentration are water quality parameters known to threaten biodiversity if they exceed certain levels (WFD UK TAG 2006, WFD UK TAG 2007). BOD_5 affects oxygen availability in rivers. Native macro invertebrate communities are often sensitive to changes in oxygen availability causing them to disappear as oxygen availability deteriorates (Carvalho *et al.* 2003). BOD_5 levels are increased by loading of organic matter such as discharges from sewage treatment works and storm overflows, and agricultural loadings from slurry and silage liquor. Elevated TN and TP concentrations can lead to increased phytoplankton growth, which can cause eutrophication and reduced biodiversity. Diatoms are sensitive to altered TN and TP concentrations and during eutrophication they are often quickly replaced by other (often undesirable) blue-green algae (Hering *et al.* 2006). Elevated TP concentrations in surface waters mainly result from sewage discharges into rivers, whereas elevated TN concentrations mainly result from agricultural practices such as manure and fertilizer application, and cultivation of N_2 fixing crops (Seitzinger *et al.* 2005).

Until recently, pollutant concentrations in surface waters were not modelled on a continental to global scale. At such scales, only pollutant loading models existed, which often treated entire river basins (e.g. Dumont *et al.* 2005), or sometimes large sub-basins as the basic unit (e.g. Grizzetti *et al.* 2008). Such models are useful for assessing the impacts of accumulation of pollutants in large water bodies at the outlets of such large (sub) basins, such as coastal shelves, lagoons or major lakes (e.g. Garnier *et al.* 2010). However, we expect that concentrations are more useful than loadings for testing of compliance with water quality standards such as those developed for the European Water Framework Directive. Many distributed (high-resolution) surface water quality models, which are suitable for modelling concentrations on the catchment to country scale, have been reported and reviewed in the scientific literature, for example by the EUROHARP project (Andersen *et al.* 2004). Such models usually require too detailed data (for input and calibration) to make application on a continental scale feasible. Nevertheless, recently three studies have been published of distributed models of pollutant concentrations on the continental scale: 1) The HYPE model (Lindström *et al.* 2010) has been used to model daily N and P concentrations across Europe on a 120 km^2 resolution. Donnelly, *et al.* (2010) validated these results by evaluating the bias of modelled long-term average concentrations (referred to as "relative volume errors") at the outlets of large European river basins. 2) The model of He *et al.* (2011), like the HYPE model, explicitly describes the terrestrial N cycle allowing the calculation of daily nitrate concentrations. Their modelled nitrate concentrations cover the whole globe on a 0.5 degree resolution, but validation only took place using multi-year average dissolved inorganic N loads (tons N $year^{-1}$) and yields (tons N km^2 $year^{-1}$) at major river basin outlets. 3) Vörösmarty *et al.* (2010) modelled long-term average BOD, N, and P concentrations on a 0.5 degree resolution in combination with 20 other geospatial drivers in order to do their global analysis of current threats to human water security and biodiversity. In their analyses they thematically grouped BOD, N, and P under “pollution” together with soil salinization, mercury deposition, pesticide loading, sediment loading, potential acidification and thermal alteration. They have not validated their modelled long-term average pollutant concentrations, but instead compared their integrated analyses of threat to human water security and river biodiversity to other threat studies.

In this paper, we would like to describe, illustrate and validate a distributed continental scale model of TN, TP and BOD concentrations which should overcome some of the shortcomings previously mentioned for existing approaches by modelling on a high spatial and temporal resolution and by validating the spatial and temporal variability of modelled concentrations (not loads). The model described in this paper is based on the GWAVA (Global Water AVailability Assessment, Meigh *et al.* 1999) model. GWAVA is a gridded model for prediction of water resources scarcity at continental and global scales. The GWAVA model has been further developed to include a water quality module. This module enables GWAVA to model concentrations of TN, TP, BOD_5, and other pollutants in a spatially distributed manner on scales ranging from the river basin scale to the global scale. In addition, the new module can be a basis for improving existing continental and global scale gridded models of water resources which are currently largely based on water quantity (e.g. Arnell 2003, Checkauer *et al.* 2003, Takata *et al.* 2003, Hanasaki *et al.* 2008) or which do not include seasonal variability (Vorosmarty *et al.* 2010).

We will validate and illustrate the current risk to human water security and biodiversity predicted by the updated GWAVA model. We developed this model such that it can be run solely using input data available for future projections (e.g. Kämäri *et al.* 2008). We also developed the model such that it is feasible to parameterise the model for pollutants which behaviour in the environment is less well known than that of TN, TP, and BOD_5.

We will first describe the pre-existing GWAVA model. Then we will describe how the updated GWAVA models levels and pathways of TN, TP, and BOD_5 from its sources (households, paved surfaces, industry, agriculture) to rivers, lakes, and wetlands. We will compare the resulting monthly gridded maps of 5-arc-minute (5') resolution of TN, TP, and BOD_5 levels with European water quality standards to indicate current aquatic biodiversity risk across Europe. Finally we will combine this with modelled human water security to provide an integrated view.

METHODS

Water flows and pollutant fluxes were modelled with a monthly time step and on a 5' grid resolution. Based on this, pollutant levels, and indicators of human water security and aquatic biodiversity were mapped across Europe. The methods used are described hereafter.

Modelling water flows with GWAVA

GWAVA is a model for prediction of water resources scarcity at continental and global scales. It was developed by Meigh *et al.* (1999) and later, it was improved and extended in different regional and global research projects (e.g. Tate *et al.* 2000, Tate and Meigh 2001, Tate *et al.* 2002, Meigh *et al.* 2005, Folwell *et al.* 2006, Farquharson *et al.* 2007, IVL *et al.* 2007). GWAVA estimates water scarcity on a cell-by-cell basis by comparing modelled river flows with modelled human demand for water (Fig. 1). First snow melt, ice melt, and rainfall interception by vegetation is modelled according to Bell and Moore (1999), Rees and Collins (2004), and Calder (1990), respectively. Then runoff from each cell is modelled with a daily time step considering vegetation, soil types and climate. The module responsible for this is largely based on the Probability Distributed Model (PDM, Moore 2007) and has been shown to be capable of producing realistic estimates of flows across Europe (Arnell

1996). Modelled cell runoff is routed through the river network including lakes, reservoirs, wetlands, and artificial water transfers such as canals. For river channels this is done using a simple Muskingum method, whereas the routing formulation for other water bodies depends on their management and use. The amount of irrigation water required by crops is modelled on a monthly basis considering 24 different crop types across pan-Europe and up to 8 crop types per cell. This irrigation water requirement is modelled as the total crop water-requirement minus the part of rainfall uptaken by the crop (effective precipitation). Total water requirement of irrigated crops is modelled according to FAO guidelines (Allen *et al.* 1998), using spatial data on irrigated areas and timing of growing seasons, and using crop factors to represent crop growth. Effective precipitation is modelled according to USDA-SCS (1970 cited by USDA-SCS 1993), based on rainfall, crop evapotranspiration, and soil water deficit. The remaining human water consumption is modelled considering annual-average population density, urbanisation, livestock density (cattle, sheep, goats), and industry. The total human water consumption is then used to model total water abstraction by considering groundwater to surface water use ratios, return flows, water supply pipe leakage, and irrigation efficiency (losses of abstracted irrigation water due to evaporation and percolation). It has recently been shown that GWAVA can well simulate runoff in natural catchments across Europe, compared to both measurements and other global hydrological models (Gudmundsson *et al.* in press).

During this study, GWAVA has been improved as follows: The calculation of irrigation water use has been refined by distinguishing between more crops and crop categories than in previous GWAVA versions. The simulation of crop growth has been extended with the possibility to vary growth season length with climate. Finally, the spatial resolution of GWAVA has been improved from 30' to 5', in order to make use of the higher resolution datasets that are currently available for Europe. Table 1 details the characteristics of the main inputs for GWAVA in this study.

Four parameters of the GWAVA rainfall-runoff module have been calibrated using river discharge measured at 110 gauges whose catchments do not overlap and cover in total about half of the modelled area (Fig 2a). This resulted in different values for the four calibration parameters in each of these 110 catchments. The four calibrated parameters affect the lateral velocity of surface and sub-surface runoff, the sub-grid distribution of soil depth, and the calculation of soil field capacity and soil saturation capacity. The measured discharge data used for calibration was for the period 1980-2000 and was provided by the Global Runoff Data Centre (GRDC 2009) and the National Centre for Atmospheric Research (NCAR, Bodo 2001). The used calibration method was Downhill Simplex in Multidimensions (Nelder and Mead 1965), which automatically searches for the parameters values leading to the best fit, according to a user-specified measure of fit. In this study, we chose to let the calibration minimize the mean absolute error (Equation (13)).

Modelling pollutant loading to surface waters

Loadings of TP, TN, and BOD_5 from land to rivers, lakes, reservoirs and wetlands are modelled as the sum of loadings from point sources and diffuse sources. Hereafter, where we use the word 'pollutant' we refer to any of TP, TN, and BOD_5.

Point source loading of any pollutant is modelled on a 5' resolution with a mass balance approach described in Williams *et al.* (accepted, 2011). This approach distinguishes point sources arising from households, industrial discharges, and runoff from paved urban areas. Pollutants from households are modelled using per-capita pollutant emissions, sewage treatment efficiencies (from Eurostat (2010) and Perry

and Venderklein (1996)), rural and urban population density (Table 1), and the fractions of the rural and urban population connected to sewage treatment works (from Eurostat (2010) and WHO/JMP (2010)). Per-capita TN and TP emissions are taken from Grizetti and Bouraoui (2006) after adjusting the per-capita TN emissions for international differences in protein levels of diets (from FAOSTAT database), and after adjusting the per-capita TP emissions for international differences in consumption of detergents containing sodium tripolyphosphate (from Glennie *et al.* (2002)). Per-capita BOD_5 emission is from IPCC (2006). Pollutants from industrial discharges are modelled using the spatial distribution of industry (from Flörke and Alcamo (2004)), its return flow and the typical pollutant concentration in this return flow (from ICPDR (2010) and a review by Williams *et al.* (accepted) of 45 literature references). In addition, removal of pollutants in treatment of industrial sewage is considered. Pollutants in runoff from paved urban areas are modelled using rainfall, urban area, population density, and reported pollutant concentrations in urban runoff (from Mitchell (2001)). We also modelled loading of pollutants from scattered settlements using the approach described in Williams *et al.* (accepted, 2011). This is modelled similarly to loading from households, except that sewage treatment levels are different.

Agricultural diffuse loading of pollutants to surface water is derived from a calibrated export coefficient method in which measured annual average pollutant load at catchment outlets was regressed against catchment characteristics. Used catchment outlets were located at water discharge monitoring stations with nearby stations monitoring TP, TN, or BOD_5 (EEA 2010b). Considered explanatory variables were catchment area, cropland area, built-up area, livestock units, Köppen–Geiger climate, lake area, river channel length, runoff, temperature, slope, point source loading, and fertilizer use of mineral and manure P and N and the atmospheric deposition of TN. Linear regression was performed using data from three time slices (1988-1992, 1993-1997, 1998-2002) during which only the significant ($p<0.05$) explanatory variables were retained. Because there were no significant differences between the regression equations generated for the different time slices, the data for all time slices were compiled together to fit a single regression equation for each pollutant (number of catchments used is 79, 106, and 104 for TN, TP, and BOD_5, resp.). The result was an equation for area specific loading at the catchment outlet for each of TP, TN, and BOD_5 having an R^2 of 0.79, 0.89, and 0.92, respectively:

$$\text{GaugeLoad}_j = c_{R,j} R + \sum_{i=1}^{m} c_{i,j} \text{Var}_{i,j} \qquad (1)$$

Here, GaugeLoad_j is the area-specific loading of pollutant *j* (TP, TN, or BOD_5) at a regression gauge (kg km^{-2} $year^{-1}$), *R* is runoff (mm $year^{-1}$) in the gauged catchment, $c_{R,j}$ is the calibrated export coefficient belonging to *R*, and $\sum_{i=1}^{m} c_{i,j} \text{Var}_{i,j}$ are the remaining *m* terms in the linear regression equation. These *m* terms include the impacts of point source emissions and agricultural activities on pollutant loading at the regression gauge (Table 2). Further explanation of equation (1) is given in Malve *et al.* (accepted).

In this study we aim to model pollutant concentrations in a spatially distributed manner. To do this, we first need an estimate of the pollutant loading to surface waters in each individual cell (as opposed to GaugeLoad_j which represents a catchment average) and subsequently we will route these pollutants through all downstream cells (as described in the next section) to estimate the pollutant concentrations for those cells. We estimated pollutant loading to surface waters by first applying Equation (1) to each individual grid cell and then correcting the resulting value for the fact that pollutant loading to surface waters happens upstream of regression gauges. Therefore the following correction was made to equation (1) when applying it to individual grid cells:

$$\text{CellLoad}_j = \alpha_j \left(c_{R,j} R + \sum_{i=1}^{m} c_{i,j} \text{Var}_{i,j} \right) \quad (2)$$

Here, CellLoad_j is the loading of pollutant *j* to surface waters from diffuse and point sources in the same cell (kg km^{-2} year^{-1}). To account for in-stream losses, it is assumed that pollutant loading from land to surface waters is on average a factor α higher then pollutant loading at the regression gauges which are further downstream. The method used to estimate α_j is explained in Appendix A. The estimated values of α_j for TN, TP and BOD_5 are very close to 1 which indicates that the effect of α_j is very small for these pollutants. However, when GWAVA will be applied to much less stable pollutants which shorter residence times then α_j will be much larger than 1. Therefore we argue that α_j is an important parameter that should be retained in the model because it allows GWAVA to be used for a wide range of pollutants.

Equation (1) was further modified as follows:

$$\text{CellLoad}_j = \alpha_j \left(c_{R,j} R + \overline{Q} \sum_{i=1}^{m} c_{i,j} \text{Var}_{i,j} \right) + S \quad (3)$$

Here, $\overline{Q}$ equals the long-term average river discharge leaving the cell (m^3 s^{-1}) if that river discharge is less than 1 m^3 s^{-1}. Otherwise $\overline{Q}$ is 1. Thus variable $\overline{Q}$ causes that the pollutant loading from land to small (<1 m^{3}s^{-1}) streams becomes more correlated to their discharge. Variables S and $\overline{Q}$ account for the sewage generated in upstream neighbouring cells with low dilution capacities (<1 m^{3}s^{-1}) that is discharged in the current cell because of its higher dilution capacity (kg km^{-2} year^{-1}). This improves the model because the Water Framework Directive prescribes that EU countries place sewage discharges at locations where the receiving waters can dilute the effluent so that it does not harm the environment (e.g. Environment Agency 2007). We estimate that sufficient dilution capacity can be expected in rivers with a discharge above approximately 1 m^{3}s^{-1}. This estimate is based on the water quality standards in Table 3, per-capita pollutant loadings to rivers estimated by Williams *et*

al. (accepted), and the fact that most people in the UK and the US are connected to sewage treatment plants serving around 13800 people (derived from Environment Agency (2008) and Michel *et al.* (1969), respectively). Variable *S* is defined as follows:

$$S = \sum_{k=1}^{n}\left(\left(1-\overline{Q}_k\right)\sum_{i=1}^{m} c_{i,j}\,\mathrm{Var}_{i,j,k}\right) \tag{4}$$

Here, *n* is the number of upstream neighbouring cells with a river discharge below 1 $m^3\ s^{-1}$ ($0 \le n \le 8$).

If the current cell and its upstream neighbours both have a discharge below 1 $m^3\ s^{-1}$ then the current cell will discharge some of the sewage produced by its upstream neighbouring cells and at the same time it will redirect a fraction ($\overline{Q}$) of the sewage produced on its own area to downstream cells. Although this representation may differ from the reality in individual grid cells, in general the use of $\overline{Q}$ and S in equation (3) resulted in more realistic modelled pollutant loadings to water. Month-to-month variability in $\mathrm{CellLoad}_j$ was obtained by using monthly values for *R*.

Modelling pollutant transport in surface waters

Pollutant concentration could be estimated by simply dividing modelled upstream pollutant loading through modelled water discharge. However, such an estimate would ignore the potentially large impact of spatial and temporal variability of drivers such as water residence time, surface water abstraction, and accumulative pollutant loss. To account for this variability, we explicitly model transport of pollutants in surface waters for each individual grid cell in pan-Europe.

The transport of pollutants after emission from point and diffuse sources is modelled by assuming that the pollutant is transported downstream with discharge through river reaches, lakes, wetlands, reservoirs, and artificial water transfers. Whist being transported downstream, pollutant may leave the river network with water abstraction. In addition, it may be lost by sedimentation and transformation. The model assumes that the latter two removal processes have rates that are proportional to pollutant concentration. Modelled values of water discharge and water abstraction are calculated by the pre-existing GWAVA model. Volumes of water in lakes, wetlands, reservoirs and river reaches are used to convert pollutant loads to concentrations and to estimate the loss and travel time of pollutants in the river network. Surface water volumes are modelled using data on land surface morphology.

We will now summarise the method used to calculate pollutant concentration. Assuming conservation of mass and complete mixing within each grid cell, the following differential equation was derived (see Appendix B for details):

$$\frac{\delta C}{\delta t} = \frac{X^{\mathrm{in}}}{V} + p_2 - C\left(\frac{Q_r + Q_a + Q_{\mathrm{tr}} + \delta V/\delta t}{V} + p_1\right) \tag{5}$$

Here, C is the pollutant concentration in a cell (kg m^{-3}), t is residence time (s), X^{in} is the pollutant loading entering the cell (kg s^{-1}), V is the surface water volume of a cell (m^3), Q_r is the river discharge leaving the cell (m^3 s^{-1}), Q_a is the abstraction of water (m^3 s^{-1}), Q_{tr} is the water outflow through artificial transfers (m^3 s^{-1}), p_1 is a loss rate constant of the pollutant due to aquatic processes such as sedimentation and transformation (s^{-1}), and p_2 is a constant production rate of the pollutant (kg m^{-3} s^{-1}) to ensure the net pollutant loss becomes zero when C reaches its pristine value. Equation (5) was solved analytically resulting in an estimate of C for every grid cell in each month of the modelled time period.

The pollutant loading into the grid cell (X^{in}) is calculated as follows:

$$X^{\text{in}} = \sum_{i=1}^{n} Q_{r,i}^{\text{in}} C_i^{\text{in}} + \sum_{k} Q_{\text{tr},k}^{\text{in}} C_k^{\text{in}} + X_t \tag{6}$$

Here, n is the number of upstream neighbouring cells ($0 \leq n \leq 8$), $Q_{r,i}^{\text{in}}$ and C_i^{in} are outgoing discharge (m^3 s^{-1}) and pollutant concentration (kg m^{-3}), respectively, in neighbouring upstream cell i, $Q_{\text{tr},k}^{\text{in}}$ is the water flux from incoming artificial transfer k (m^3 s^{-1}) and C_k^{in} is the concentration in the grid cell where transfer k is coming from (kg m^{-3}). Variable X_t is the pollutant loading from diffuse and point sources in the cell (kg s^{-1}), which is modelled using equation (3).

The surface water volume of a cell (V) can comprise both river reaches (V_r) and an impoundment such as a lake, reservoir or wetland (V_l). Therefore, V is calculated as:

$$V = V_r + V_l \tag{7}$$

Volume V_l is calculated as follows:

$$V_l = V_L \cdot \frac{1 - f_{\text{land}}}{\sum_{i=1}^{L} \left(1 - f_{\text{land},i}\right)} \tag{8}$$

Here, V_L is the total volume of the lake, reservoir or wetland calculated for each time step by the pre-existing GWAVA, L is the total number of cells covered by the same lake, reservoir or wetland as the current cell, $f_{\text{land},i}$ is the fraction of land in cell i that is not covered by the lake, reservoir, or wetland, and f_{land} is the fraction of land in the current cell that is not covered by the lake, reservoir or wetland.

Variable V_r is calculated as:

$$V_r = d \cdot w \cdot l \cdot f_m \cdot f_{\text{land}} \tag{9}$$

Here d is river depth (m), w is river width (m), l is the river length without meandering (m), and f_m is a meandering factor defined as actual river length divided by l.

River width, w, is estimated using grid-cell discharge according to Allen *et al.* (1994). Meandering factor, f_m, is calculated as a function of grid-cell size according to Fekete *et al.* (2001). River depth, d, is calculated according to Pistocchi and Pennington (2006):

$$d = w^{-0.6} \cdot \overline{Q}_r^{0.6} \cdot s^{-0.3} \cdot 0.045 \quad (10)$$

Here s is river bed slope estimated from drainage network topography and the sub-grid cell (30" resolution) elevation distribution, 0.045 is a river bed roughness value representative for Europe (unitless), and $\overline{Q}_r$ is the average of river discharge entering and leaving the cell ($m^3\ s^{-1}$).

The values of p_1 (equation (5)) have been calibrated with measured pollutant concentrations from EEA (2011a) for the period 1990-2000. This calibration was done manually by adjusting p_1 to minimize the difference between the median of all modelled pollutant concentrations across the EU, and the median of all measured concentrations across the EU. We calibrated p_1 because literature values of pollutant loss rates are usually only validated for specific surface water types or expressed in incomparable units (Birgand *et al.* 2007).

Production rate p_2 was estimated as:

$$p_2 = p_1 \cdot C_{\text{nat}} \quad (11)$$

Here C_{nat} is an estimated natural background concentration for the modelled pollutant (kg m^{-3}). Equation (11) is derived from equation (5) and the following three assumptions about cells in natural river systems: (1) Inflowing water has the same natural pollutant concentration as outflowing water, (2) X_t is zero, and (3) concentration change over time is negligible (i.e. $\delta C/\delta t \approx 0$). The first and second assumption cause pollutant loading into the cell to equal the sum of the pollutant storage rate and the pollutant flux out of the cell (i.e. $X^{\text{in}} = C\left(Q_r + Q_a + Q_{\text{tr}} + \delta V/\delta t\right)$). The consequence of this and the third assumption is that aquatic production of the pollutant (p_2) equals aquatic loss of the pollutant ($p_1 \cdot C_{\text{nat}}$). We acknowledge that the third assumption may ignore some seasonal variation. However, this is acceptable in this study as the focus is on human influenced systems with possible risk of eutrophication where most of the variation in C is driven by anthropogenic pollution and its dilution and transport. The C_{nat} that was used for BOD_5 was the first percentile of the measured concentrations across Europe from EEA Waterbase (EEA 2010b) and the C_{nat} values for TN and TP were based on Smith *et al.* (2003).

Risk indices

One of the aims of the present study is to indicate the human water security risk. For this we use an index that considers both the human demand for water and the availability of water. This index is GWAVA's Water Availability Index 4 (WAI4):

$$\mathrm{WAI4} = \min\left(\frac{\mathrm{avail10}_i - \mathrm{dem}_i}{\mathrm{avail10}_i + \mathrm{dem}_i}; i = 1,2,...,12 \right) \quad (12)$$

Here, $\mathrm{avail10}_i$ is the multi-annual 10th percentile water availability ($m^3\ s^{-1}$) for month i, and dem_i is the multi-annual average human water demand ($m^3\ s^{-1}$) for month i. Here, the term 'multi-annual' indicates that the percentile or average is based on as many values as there are years in the modelled time period. WAI4 is between 0 and 1 in cells with sufficient water resources to satisfy the local demand for water. If WAI4 is between 0 and -1 then water scarcity is expected to occur regularly (more than once in 10 years) if there is no water supply infrastructure that can transfer water over large distances (further than the grid cell radius). If such infrastructure is present then a WAI4 between 0 and -1 indicates that future climate change or future water demand growth may cause the need to extend this infrastructure further into neighbouring regions, or to build new water supply reservoirs which can store excess water during wet months for release during dry months.

We calculated risk for aquatic biodiversity using European standards aimed at conservation of biodiversity. We assumed that biodiversity is at risk if either BOD_5, TN, or TP levels are above the critical levels prescribed by these standards. The critical levels that we used (Table 3) are developed to test compliance with the European Water Framework Directive (WFD) and Nitrates Directive. The UK Technical Advisory Group on the WFD (UK TAG) provides critical 90th percentile BOD_5 levels for rivers, and critical mean soluble reactive phosphorus (SRP) levels for lakes and rivers (UK TAG 2006, UK TAG 2007). UK TAG gives different critical levels for different types of lakes and rivers because the native biota living in these types have different sensitivities to BOD_5 and SRP. We took the median over these different types and converted SRP levels to TP levels according to Bradford and Peters (1987). The critical levels from UK TAG (2006, 2007) which we used for BOD_5 and TP are those which are exceeded in only 10% of 'healthy' aquatic ecosystems, where even the most sensitive biological element (macro-invertebrates) is still undisturbed. Critical levels for TN were from Król and Sokół (2006) who developed these levels for implementation of the EU nitrates directive. Their critical TN levels are those above which eutrophication, and thus deterioration of biodiversity, starts to occur. The standards for stagnant waters (Table 3) were applied if more than 1% of the cell area is covered by lakes and wetlands according to the CCM2 database (Vogt *et al.* 2007). Otherwise we applied the critical levels for running waters (Table 3). We only indicate risk for biodiversity where the modelled water volume per cell (equation (7)) is more than zero in all modelled months. Cells where this is not the case are unlikely to have point source loading that is continuous, which would be a violation of one of our model assumptions.

Modelled time scales

All input data used in the modelling, except climatic input, represent the year 2000. Climatic input was monthly[1] data from 1960 to 2000, of which the first 30 years were used for model warm-up. The index of risk for biodiversity is simulated using month-to-month variability in hydrology and pollutant concentrations resulting from variability in climate input from 1990 to 2000. The human water security index (WAI4) is based on month-to-month variability in hydrology and human water demands in the period from 1970 to 2000.

Model fit

Fit of modelled river discharge is indicated for 110 calibration gauges, both after and before calibration. The fit before calibration results from using default values for the four calibration parameters of the rainfall-runoff module in the 110 calibration catchments. This fit is indicative of the quality of modelled discharge in the catchments that were not calibrated. Default values for the four calibration parameters of the rainfall-runoff module are in the middle of the range of plausible values.

Fit of modelled pollutant concentrations is demonstrated in detail with plots of modelled versus measured concentrations for many locations, whereas fit of water discharge will be summarized using three indices of fit. The reasons for this more elaborate assessment of modelled pollutant concentrations is that pollutant modelling is a new feature of GWAVA that has not been published before, whereas validations of GWAVA modelled water discharge have already been described in numerous other publications.

Model fit is indicated with three different measures, each indicating a different characteristic of the model fit. The first measure is the mean absolute error:

$$\bar{e}_{\text{abs}} = 100 \cdot \frac{\sum_{i=1}^{n} \left| \text{mod}_i - \text{obs}_i \right|}{\sum_{i=1}^{n} \text{obs}_i} \qquad (13)$$

Here, $\bar{e}_{\text{abs}}$ is the mean absolute error (%), n is the number of used observations, obs_i is an observation, and mod_i is a model prediction. We use $\bar{e}_{\text{abs}}$ to indicate model fit because it is relatively sensitive to errors in predicted discharge during dry periods (Krauze *et al.* 2005). This is important because our WAI4 index is sensitive to months with low discharge, and because lower discharge can cause higher pollutant concentrations to which the biodiversity risk index is sensitive.

Secondly, we used the model bias:

$$\Delta\mu = 100 \cdot \frac{\mu_{\text{mod}} - \mu_{\text{obs}}}{\mu_{\text{obs}}} \qquad (14)$$

[1] GWAVA downscales climate input to daily resolution for rainfall-runoff modelling.

Here μ denotes the arithmetic mean and the indices obs and mod indicate observed and modelled values, respectively.

Finally we quantified the model's ability to capture the temporal patterns of variability using Spearman's correlation coefficient *r*.

RESULTS AND DISCUSSION

Model performance

Fig. 3 illustrates the capability of GWAVA to simulate river discharge for a large calibrated river basin which is roughly in the centre of Europe: the Meuse river (near Lith, Netherlands). We chose the Meuse to allow comparison with Fig. 4 which shows water quality in the Meuse. For other calibrated rivers in Europe, the fit of modelled discharge is given in Table C1 (Appendix C). The mean absolute error in these rivers is about 21% lower than in uncalibrated rivers (Table C1). Modelled discharge has a low fit for many rivers in Iceland, Norway and Finland. This is likely to be due to some simplifications in GWAVA's snowmelt module, especially the assumption snowmelt is driven by temperature and but not radiation. However, the main reason for this low fit is probably that the snowmelt module was not calibrated for this study.

The spatial variability of modelled BOD_5, TN and TP concentrations is compared to the spatial variability of measured concentrations in the Meuse river (Fig. 4). The Meuse was chosen for this comparison as it has many suitable monitoring stations (EEA 2010b), and because the values of many of its watershed properties (e.g. latitudes, slopes, point source emissions, agricultural intensities) are in the middle of the range of values that can be found in the rest of Europe. However, as in most river basins, there are not many stations with overlapping periods of measurement within 1990-2000. For most stations in the Meuse, measured annual data was available for the years around 1999. Therefore, we only used measured concentrations from years close to 1999 for this validation of modelled spatial variability. The fit of modelled spatial variability in the Meuse was best for BOD_5 ($\bar{e}_{abs}$ = 16 %) and worst for TP ($\bar{e}_{abs}$ = 24 %). The general trend in the measured TN and TP concentrations along the Meuse (slight decrease from 300 to 3000 km^2 upstream area followed by steep increase from 3000 to 30000 km^2 upstream area) is reproduced by the model (r = 0.91 and 0.82, respectively). The average concentration in the Meuse is modelled well for TP and BOD_5 ($\Delta\mu$ = -6 and -7%, respectively). For all three pollutants, the spatial autocorrelation of the measured values is lower than the spatial autocorrelation of the modelled values. This may be caused by the fact that measurement times do not exactly match between different stations along the Meuse, whereas the modelled concentrations for those stations represent exactly the same time period. In addition, the exaggerated spatial autocorrelation may stem from real-world local processes that are not included in the model.

The validation of modelled temporal variability of pollutant concentrations is shown for 24 stations (Fig 2b) selected from EEA Waterbase-rivers version 11 (EEA 2011a). The values reported in this database are measured concentrations which are aggregated seasonally or annually, although for most countries the database has only annual values. One station was selected for each country represented in the EEA database, except for countries lacking suitable stations. Within each country, the station with the largest catchment area and the highest number of measured seasons

was chosen if this station had at least three years of data in the 1990-2000 period. Annual data values were only used if they were based on at least ten samples, and seasonal values were only used if they were based on at least four samples. Some countries (e.g. Bosnia Herzegovina) had no station with at least three years of data values based on sufficient samples. Therefore these countries are not used in our assessment of fit of modelled pollutant concentrations. The correlation between measured and modelled pollutant concentrations depends very much on the number of samples on which the measured concentrations were based. For example, relatively high correlations were found in station Kleve-Bimmen (Rhine river) where the number of samples per data value was very high (Fig. 5 to 7). Concentrations near the mouths of large river basins are generally underestimated (Fig. 5 to 7). This is likely to be due to the fact that parameter p_1 was calibrated such that modelled concentrations in most grid cells have a low bias, whereas river reaches as large as those of the selected 24 water quality measurement stations (Fig. 2b) cover only a very specific category of the grid cells.

The fit of modelled concentrations on the pan-European scale is not as good as can be expected on smaller scales (such as the scale of an individual catchment) where it is possible to parameterize more complex models using more detailed local information. However, such detailed data is not available on the scale of this study.

The fit of calibrated and validated river discharges is generally better than the fit of modelled pollutant concentrations. One reason is that modelling of pollutant concentrations relies on modelled hydrological variables, such as river discharge. Thus any uncertainty in this modelled hydrology is added to the uncertainty in modelled pollutant concentrations. Especially, the relative uncertainty in dry-month discharge is important because pollutant concentration has a reciprocal relationship with dilution capacity. Another reason for the relatively low fit of pollutant concentrations compared to discharge is that measured concentrations in many river basins show decreasing trends during the modelled period. These decreasing trends, which are probably the result of quick-changing mitigation measures, are not reproduced by the model. For example, pollutant management has caused a marked fall in nitrate concentrations in Denmark, Germany, and Latvia during the 1990-2000 period (EEA 2010a). Modelled concentrations are also affected by model simplifications such as those used to model pollutant loading from point sources (Williams *et al.* accepted). In this method the most important simplifications are i) the use of a typical pollutant concentration in industrial return flow, ii) the assumption that this return flow has been treated in all countries, iii) the use of the same removal efficiencies for sewage treatment works of the same type in all countries (leading to errors especially because we do not know which sewage treatment works have nutrient removal), and iiii) the assumption that households that are not connected to sewerage systems have good local treatment (secondary level).

Modelled concentrations are affected by uncertainties in the used export coefficient equation for diffuse pollutant loading (Malve *et al.*, accepted). In this model the most important uncertainties are i) that not all areas in Europe were equally represented when fitting the export coefficient equation, ii) that the number of water quality observations was low for some catchments used in this fitting (for some catchments as little as six measurements per year), and iii) that the export coefficient equation uses cropland area and livestock numbers as surrogates for agricultural input of mineral fertilizers and manure from livestock, respectively. The export coefficient method (equation (1)) on which pollutant loading to surface waters was based has been validated by Malve *et al.* (accepted). They did this by developing an export

coefficient equation for 3 different time periods (1988-1992, 1993-1997, 1998-2002) and 3 different sets of observed catchments, and showed that the resulting equations are not significantly different from each other and from equation (1). This indicates that equation (1) is valid in time periods and locations that were not used for its calibration.

Finally, the another important source of uncertainty is the decay-coefficient p_1 which is spatially and temporally constant causing that the modelled patterns exhibit less variability then the measured patterns (evident in Fig. 4 to 7).

Modelled water security risk across Europe

GWAVA predicts that current risk for human water security is concentrated in Mediterranean, arid and densely populated parts of Europe (WAI4<0 in Fig. 8). The spatial pattern of water security risk appears to be mainly determined by population density and climate. In regions with warm climates having dry and warm summers (south of the Iberian peninsula, Greece, most of Turkey, Cypress, Sardinia, Sicily, Israel, and the Mediterranean coasts of Spain, France and Italy), water security risk is already indicated at moderate population densities (> 25 inhabitants km^{-2}) and in a few areas with very high irrigation water abstraction (>100 mm year, especially in the south of Spain). However, in regions further north, which have a more humid climate, water security risk is only indicated in areas that are predominantly urban (>425 inhabitants km^{-2}). Examples of such areas can especially be found near the large cities in the west of Germany, the Netherlands and Belgium, and in the southern half of the UK. In the extreme south east of the modelled area, where arid climates dominate, water security risk is indicated even at extremely low population densities. Further, GWAVA indicates some risk for human water security in wetland dominated parts of Scandinavia due to GWAVA's assumption that swamps cannot be used for water abstraction.

The modelled human water security across Europe generally looks plausible as it corresponds well with human water stress modelled on a similar scale by the WaterGAP model (Alcamo 2003). However, the water security risk may have been exaggerated in the wealthier regions of pan-Europe, because our risk indicator does not include the financial and technical means of local water resources managers to extend their water supply infrastructure across cell boundaries, nor does it include their means to reduce water demand by measures such as hosepipe bans or water price increases. In the dryer parts of Europe, the water security risk may have been locally exaggerated because we did not use GWAVA's module for simulating large water transfers (e.g. transfers from large water-supply reservoirs to users in different cells) and artificial water courses across basin divides. The reason for this is the absence of a suitable dataset of such structures on the pan-European scale. Moreover, this study may have exaggerated water security risk because long-term storage of water in deep aquifers was not modelled (the model only has a shallow groundwater store) and thus some regions for which water security risk was indicated may in fact draw heavily on deep groundwater to compensate for lack of surface water. This is, for example, the case for Germany and Denmark (EEA 2005 cited by Furberg *et al.* 2006). However regions extensively exploiting their groundwater run the risk of lowering their groundwater table or of causing saltwater intrusion (as is often the case in the Mediterranean region). In such regions the indicated water security risk is more a signal that there is an unsustainable rate of water abstraction which may cause actual water stress in the future. The last reason why water security risk may have been

exaggerated is that our input data on reservoirs (Table 1) only includes relatively large reservoirs. Thus the effect of smaller reservoirs on reduction of water security risk may not have been accounted for.

Modelled pollutant concentrations across Europe

Across Europe, high modelled pollutant concentrations can be found in areas with intensive agricultural activities, such as the Po valley and the lowlands of the Netherlands and Belgium. On the other hand, low modelled concentrations occur in regions with little human influence, such as the Alps and Scotland. In addition, low pollutant concentrations are generally modelled in parts of Europe with large lakes and wetlands, such as Scandinavia, due to their long water residence times which increase decay of pollutants. Finally, the modelled pollutant concentrations may either increase or decrease in downstream direction, depending on the degradability of the pollutant, and the spatial patterns within the river basin of hydrology and pollutant sources.

Fig. 9 shows that high TP concentrations are modelled especially in Israel, Belgium, and Portugal. In Israel and Portugal, this is mainly due to high evapotranspiration rates leading to low river discharge limiting the dilution of point source pollutants, whereas the high TP concentrations in Belgium are mainly due to scattered settlements. High TP concentrations in many Eastern European rivers are modelled because of relatively low precipitation causing lower dilution capacity of these rivers. High TN concentrations are modelled along the Atlantic Ocean in Western and Southern Europe, and in the Po basin. The reasons for high TN concentrations along the Atlantic Ocean in Western and Southern Europe are similar to those previously mentioned for TP, but in addition livestock is an important reason for high TN concentrations in the Netherlands, western France, western England and eastern Ireland. In the Po basin, high TN concentrations are mainly caused by emissions from cropland and scattered settlements. Fig. 9 indicates that high BOD_5 concentrations can be found in Belgium. This is due to high livestock densities and high emissions from scattered settlements. High modelled BOD_5 concentrations are also common in Serbia Montenegro and Israel due to high emissions from manufacturing.

The modelled concentrations across Europe look plausible given the spatial distribution of pollutant sources (mainly human population and livestock), dilution capacity (discharge), and sinks (mainly lakes, wetlands, and big river reaches). Furberg *et al.* (2006) shows the location of regions with relatively high and relatively low measured N and P concentrations throughout Europe. This matches well with some regions in Europe where GWAVA predicts that both TN and TP are relatively high (south-west of the Iberian peninsula, Meuse and Scheldt basin, South-England). However, comparison with Furberg *et al.* (2006) indicates that there are also some regions where GWAVA underestimates TN or TP concentrations (Bulgaria, Poland, Latvia). The modelled lake TP and river BOD_5 levels (Fig. 9) are generally consistent with those reported in the Water Information System for Europe (WISE) (EEA 2011b). The differences (higher modelled BOD in the Netherlands, and lower modelled BOD in the south of Italy) can be explained by the fact that the WISE database is more representative for the situation after the year 2000, whereas our model results cover the period 1990-2000.

Modelled aquatic biodiversity risk

Modelled concentrations indicate aquatic biodiversity risk in about 35% of the European area, especially where lakes and wetlands are abundant (Fig. 10). Modelled biodiversity risk in about 67% of the affected areas is solely due to high TP concentrations. The reason why much of Scandinavia is modelled to have aquatic biodiversity risk (Fig. 10) is that lake cover exceeds 1% in about half of the Scandinavian cells. Therefore, the stricter TP standard for stagnant waters (Table 3) applies there. The number of cells where TN standards are not met is about 58% smaller than where the TP standards are not met, and they largely coincide with cells where TP standards are not met. The number of cells where BOD_5 standards are not met is about 87% smaller than where the TP standards are not met, although their spatial distribution is different. In contrast to TP, BOD_5 standards are not met in large proportions of the Caucasus region and in Serbia-Montenegro, making BOD_5 the main cause of aquatic biodiversity risk in those regions.

Our result that aquatic biodiversity risk is mostly caused by too high TP concentrations is corroborated by numerous other published studies indicating that TP is the most common driver behind freshwater eutrophication (e.g. Guildford *et al.*, 2000). The combined spatial pattern of indicated risk for biodiversity and human water security agrees with local studies identifying similar risks (SCENES 2008) and with spatial modelling of similar risks done by Vörösmarty *et al.* (2010).

The presented method

Generally, the model results look good and plausible. Validation showed that the developed modelling method can predict the spatial variation of modelled concentrations. However, the temporal variability of concentrations is only modelled well in a proportion of the river basins. Therefore, future model improvements should focus on this modelled temporal variability. GWAVA modelled concentrations and flows have not been corrected with measurements, thus allowing model errors to propagate downstream. Such corrections were not applied in order to allow the model to be applied for prediction of the future for which measured concentrations and flows are obviously not available.

When interpreting the indicated biodiversity risk and water security risk, it should be kept in mind that no indicator can capture all factors that affect these risks. Instead the indicators are intended to provide a broad picture of risk which is based on a few very important drivers which are likely to be dominant in many locations.

We suggest that the enhanced GWAVA version presented in this paper could benefit river basin management plans (RBMPs) which are implemented throughout the European Union as prescribed by the Water Framework Directive. The new GWAVA version can assess whether the water quality objectives of RBMPs are sustainable in the long term given long term changes in the climate, economy and population distribution. Also it allows assessment of possible conflicts that may arise between water quality objectives in RBMPs and the water needs of the human population.

The fact that the net pollutant loss in surface waters only depends on parameters p_1 and C_{nat} makes it feasible to parameterise the model for pollutants which fate and behaviour in the environment is not yet very well known, as is often the case for newly developed chemicals. This makes our model potentially useful for environmental risk assessments of new chemicals (European Chemicals Agency 2008).

CONCLUSION

We developed a spatially and temporally explicit model of human water security, and water pollution. This model represents a substantial proportion of measured spatial and temporal variability in measured river discharge and levels of TN, TP and BOD_5 in rivers on the pan European scale. However, there is scope for improvement, especially in the representation of the temporal variability of concentrations. Deviations of model results from published statistics of TN, TP and BOD_5 levels can be explained by uncertainty in these statistics due to low sampling frequencies. Another reason is the relatively low complexity of the water quality module to allow for parameterization of many different pollutants on a scale as large as pan Europe. In general, however, the model results look good and plausible.

The developed model can account for changes in a comprehensive set of driving forces including drivers such as climate, population, damming, cropping patterns, and commitments to wastewater treatment. It thus enables integrated water resources managers to better assess the effects of anticipated changes.

The results of the developed model show that water security risk and biodiversity risk are likely where the population density is high, the agriculture is intensive, the climate is dry, and lakes or wetlands are abundant.

Future use of the presented method will include modelling of future scenarios and additional pollutants.

Acknowledgements We thank the SCENES project from the European Commission (FP6 contract 036822) for funding the research that resulted in this paper. Also, we thank GRDC for providing most of the data needed for calibration of modelled river discharge.

APPENDIX A

The values of α_j (equation (2)) were estimated by first assuming that the loss of pollutants in the river network of most regression catchments is dominated by aquatic loss processes such as sedimentation and transformation. Secondly, we assumed that this river network loss can be approximated using an analogy with a long unbranched channel consisting of many well-mixed subsections, such that the loss in each of these subsections can be described as

$$\frac{\delta C_s}{\delta t} \approx -p_1 C_s \qquad \text{(A1)}$$

Here, C_s is the pollutant concentration in a subsection (kg m^{-3}), t is residence time (s), and p_1 is a loss rate constant of the pollutant due to aquatic processes such as sedimentation and transformation (s^{-1}). A solution of equation A1 can be expressed as follows:

$$C_s^{\text{out}}(t+\Delta t, x) = C_s^{\text{in}}(t, x) \cdot \mathrm{e}^{-p_1 \cdot \Delta t} \qquad \text{(A2)}$$

Here, Δt is the time needed for the pollutant to travel through a subsection (s), x is the number of the current subsection (starting at 1 and increasing in downstream direction until $x_{\max}$), $C_s^{\text{out}}(t+\Delta t, x)$ is the pollutant concentration in the river water flowing out of subsection x (kg m^{-3}), and $C_s^{\text{in}}(t,x)$ is the pollutant concentration in the river water flowing into subsection x (kg m^{-3}). Variable $C_s^{\text{in}}(t,x)$ is calculated as:

$$\begin{aligned} C_s^{\text{in}}(t,x) &= \frac{\text{PollLoad}}{Q_s(x)} && \text{if } x=1 \text{ and } t=0 \\ C_s^{\text{in}}(t,x) &= \frac{Q_s(x-1)\cdot C_s^{\text{out}}(t,x-1)+\text{PollLoad}}{Q_s(x)} && \text{if } x>1 \text{ and } t_{\max} \geq t \geq \Delta t \end{aligned} \quad \text{(A3)}$$

Here, PollLoad is the pollutant loading from diffuse and point sources into each subsection (kg s^{-1}), and $Q_s(x)$ is the river discharge in subsection x (m^3 s^{-1}). We assume that PollLand is the same for all subsections, and that $Q_s(x)$ is proportional to x. Both $Q_s(x)$ and PollLand are assumed to be constant in time. Using these assumptions, we can iteratively apply equations A2 and A3, starting at x=1 and ending with $x_{\max}$. This results in the value of $C_s^{out}(t_{\max}, x_{\max})$ which represents the concentration at a regression gauge. The values of $x_{\max}$ and Δt are chosen such that:

$$\Delta t = t_{\max} / x_{\max} \quad \text{(A4)}$$

The value chosen for $t_{\max}$ is 67000 s, which is the expected travel time of the pollutant to the corresponding regression gauge. This value is based on cell travel times estimated as the ratio of modelled V to modelled Q_r (defined below equation (5)) for individual cells in the regression catchments.

Equations A2, A3, and A4 allow us to estimate α_j as:

$$\alpha_j = \frac{x_{\max}\cdot \text{PollLand}}{C_s^{\text{out}}(t_{\max}, x_{\max})\cdot Q_s(x_{\max})} \quad \text{(A5)}$$

Here, the numerator represents CellLoad$_j$ and the denominator represents GaugeLoad$_j$. The estimated value of α_j does not depend value of PollLand and the ratio of $Q_s(x)$ to x. Thus it only depends on the value chosen for p_1.

APPENDIX B

Derivation of equation (5) is based on a similar approach used in the derivation of the QUESTOR model (Eatherall *et al.* 1998). The following equation describes the mass balance of a pollutant in a grid cell while assuming complete mixing.

$$\frac{\delta(CV)}{\delta t} = X^{\text{in}} + p_2 V - C(Q_r + Q_a + Q_{\text{tr}}) - p_1 CV \qquad \text{(B1)}$$

Here, C is the pollutant concentration in a cell (kg m^{-3}), V is the surface water volume of a cell (m^3), t is residence time (s), X^{in} is the pollutant loading entering the cell (kg s^{-1}), Q_r is the river discharge leaving the cell (m^3 s^{-1}), Q_a is the gross abstraction of water (m^3 s^{-1}), Q_{tr} is the water outflow through artificial transfers (m^3 s^{-1}), p_1 is a loss rate constant of the pollutant due to aquatic processes such as sedimentation and transformation (s^{-1}), and p_1 is a constant production rate of the pollutant (kg m^{-3} s^{-1}) to ensure the net pollutant loss becomes zero when C reaches its pristine value.

From the product rule follows that

$$\frac{\delta(CV)}{\delta t} = V\frac{\delta C}{\delta t} + C\frac{\delta V}{\delta t} \qquad \text{(B2)}$$

Combining equations (B1) and (B2) gives

$$X^{\text{in}} + p_2 V - C(Q_r + Q_a + Q_{\text{tr}}) - p_1 CV = V\frac{\delta C}{\delta t} + C\frac{\delta V}{\delta t} \qquad \text{(B3)}$$

Rearrangement of equation (B3) gives equation (5)

APPENDIX C

REFERENCES

Alcamo, J., Märker, M., Flörke, M. and Vassolo, S., 2003. *Water and Climate: A Global Perspective.* Kassel, Germany: CESR, Kassel World Water Series, Report nr. 6.

Allen, P. M., Arnold, J. G., and Byars, B. W., 1994. Downstream channel geometry for use in planning-level models. *Water Resources Bulletin*, 30 (4), 663–671.

Allen, R. G., Pereira, L. S., Raes, D. and Smith, M., 1998. *Crop evapotranspiration - Guidelines for computing crop water requirements.* Rome: FAO, FAO Irrigation and drainage paper 56. Available from: http://www.fao.org/docrep/X0490E/X0490E00.htm [Accessed 12 March 2012].

Andersen, H.E., *et al.*, 2004. *Modelling approaches: Model parameterisation, calibration and performance assessment methods in the EUROHARP project.* Oslo: NIVA, EUROHARP 8-2004.

Arnell, N. W., 1996. *Global Warming, River Flows and Water Resources.* Chichester: Wiley.

Arnell, N.W., 2003. Effects of IPCC SRES emissions scenarios on river runoff: a global perspective. *Hydrology and Earth System Sciences*, 7 (5), 619–641.
Balk, D. and Yetman, G., 2004. *The Global Distribution of Population: Evaluating the Gains in Resolution Refinement.* Palisades, NY: CIESIN.
Bates, B. C., Kundzewicz, Z. W., Wu, S. and Palutikof, J. P., 2008. *Climate change and water.* Geneva: IPCC Technical paper.
Bell, V.A. and Moore, R.J., 1999. An elevation-dependent snowmelt model for upland Britain. *Hydrological Processes*, 12, 1887-1903.
Billen, G., Beusen, A., Bouwman, L., Garnier, J., 2010. Anthropogenic nitrogen autotrophy and heterotrophy of the world's watersheds: Past, present, and future trends. *Global Biogeochemical Cycles*, 24, Doi 10.1029/2009gb003702
Birgand, F., Skaggs, R. W., Chescheir, G. M. and Wendell, G. J., 2007. Nitrogen Removal in Streams of Agricultural Catchments—A Literature Review. *Critical Reviews in Environmental Science and Technology*, 37 (5), 381—487.
Bodo, B.A., 2001. *Annotations for monthly discharge data for world rivers (excluding former Soviet Union).* Boulder, CO: NCAR. Available from http://dss.ucar.edu/datasets/ds552.1/docs/
Bradford, M.E. and Peters, R.H., 1987. The relationship between chemically analyzed phosphorus fractions and bioavailable phosphorus. *Limnology And Oceanography*, 32 (5), 1124-1137.
Calder, I.R., 1990. Evaporation in the Uplands. Chichester: Wiley.
Carvalho, L., *et al.*, 2003. Physico-chemical conditions for supporting different levels of biological quality for the Water Framework Directive for freshwaters. London: Environment Agency.
Cherkauer, K.A., Bowling, L.C. and Lettenmaier, D.P., 2003. Variable infiltration capacity cold land process model updates. *Global and Planetary Change*, 8 (1-2), 151-159.
CLC2000, 2009. Corine Land Cover 2000 100 m, Version 12/2009. Copenhagen: European Environment Agency. Available from http://www.eea.europa.eu/data-and-maps/data/corine-land-cover-2000-clc2000-100-m-version-12-2009.
De Smedt, F., 1989. Introduction to river water quality modeling. Brussels: VUB press.
Dearmont, D., McCarl, B., and Tolman, D., 1998. Costs of Water Treatment Due to Diminished Water Quality: A Case Study in Texas. *Water Resources Research*, 34 (4), 849-853.
Donnelly, C., Dahné, J., Strömqvist, J., and Arheimer, B., 2010. Modelling Tools: From Sweden to Pan-European Scales for European WFD Data Requirements. *In: BALWOIS 4th international conference,* 25-29 May 2010 Ohrid, Macedonia.
Dumont, E., *et al.*, 2005. Global distribution and sources of dissolved inorganic nitrogen export to the coastal zone: Results from a spatially explicit, global model. *Global Biogeochemical Cycles*, 19, GB4S02, doi:10.1029/2005GB002488.
Eatherall, A., Boorman, D.B., Williams, R.J., and Kowe, R., 1998. Modelling in-stream water quality in LOIS. *Science of the Total Environment*, 210/211, 499–518.
Environment Agency, 2006. Pollution prevention guidelines. Treatment and disposal of sewage where no foul sewer is available: PPG4. London, Environment

Agency. Available from: http://publications.environment-agency.gov.uk/pdf/PMHO0706BJGL-E-E.pdf
Environment Agency, 2008. Catchment Risk Assessment of Steroid Oestrogens from Sewage Treatment Works. London, Environment Agency. Science Report SC030275/SR3. ISBN: 978-1-84432-871-0
EEA, 2010a. *Nutrients in freshwater (CSI 020).* Copenhagen: European Environment Agency. Available from: http://www.eea.europa.eu/data-and-maps/indicators/nutrients-in-freshwater/nutrients-in-freshwater-assessment-published-4 [Accessed November 2011].
EEA, 2010b. *Waterbase - Rivers, version 10.* Copenhagen: European Environment Agency. Available from: http://www.eea.europa.eu/data-and-maps/data/waterbase-rivers-6.
EEA, 2011a. *Waterbase - Rivers, version 11.* Copenhagen: European Environment Agency. Available from: http://www.eea.europa.eu/data-and-maps/data/waterbase-rivers-7.
EEA, 2011b. *Water Information System for Europe (WISE).* Copenhagen: European Environment Agency. Available from http://www.eea.europa.eu/highlights/themes/water/interactive/soe-rl
European Commission, 2010. Eurostat database. Luxembourg, Eurostat. Available from: http://epp.eurostat.ec.europa.eu/portal/page/portal/eurostat/home
European Chemicals Agency, 2008. Environmental Exposure Estimation. *In: Guidance on information requirements and chemical safety assessment.* Helsinki: European Chemicals Agency.
FAO *et al.*, 2009. *Harmonized World Soil Database (version 1.1).* Rome: FAO, and Laxenburg, Austria: IIASA.
Farquharson, F.A.K., *et al.*, 2007. *Impact of Climate and Sea Level Change in part of the Indian Sub-Continent.* London: DFID, Project R8038.
Fekete, B.M., Vörösmarty, C.J., and Lammers, R.B., 2001. Scaling gridded river networks for macroscale hydrology: Development, analyses, and control of error. *Water Resources Research*, 37 (7), 1955-1967.
Flörke, M. and Alcamo, J., 2004. *European Outlook on Water Use.* Copenhagen: European Environment Agency, Final Report, EEA/RNC/03/007
Folwell, S.S. and Farquharson, F.A.K., 2006. The Impacts of climate change on water resources in the Okavango Basin. *In: Climate variability and change: hydrological impacts. 5th World FRIEND Conference*, November 2006 Havana. Wallingford, UK: IAHS Press, Publication No. 308, 382-388.
Furberg, D., Nilsson, S., and Langaas, S., 2006. An indicator-based analysis of the river basin districts established under the EU Water Framework Directive. *E-WAter* [online], Article no. 2006/18. Available from: http://www.dwa.de/portale/ewa/ewa.nsf/home?readform&objectid=0AB6528C5177A8B7C12572B1004EF1C7&editor=no&&submenu=_1_6_2&&treeid=_1_6_2&
Garnier, J., *et al.*, 2010. N:P:Si nutrient export ratios and ecological consequences in coastal seas evaluated by the ICEP approach. *Global Biogeochemical Cycles*, 24, GB0A05, doi:10.1029/2009GB003583.
Glennie, E.B., *et al.*, 2002. *EU Environment Directorate. Phosphates and alternative detergent builders – Final report.* Swindon, UK: WRc, Report No.: UC 4011.
GRDC, 2009. *Global Runoff Data Centre.* Koblenz, Germany: Federal Institute of Hydrology. Available from: http://www.bafg.de/GRDC.

Grizzetti, B. and Bouraoui, F., 2006. *Assessment of Nitrogen and Phosphorus Environmental Pressure at European Scale.* Ispra, Italy: Joint Research Centre.

Grizzetti, B., Bouraoui, F., and De Marsily, G., 2008. Assessing nitrogen pressures on European surface water. *Global Biogeochemical Cycles* **22**. 1-14.

Gudmundsson, L., *et al.*, in press. Comparing large-scale hydrological model simulations to observed runoff percentiles in Europe. *Journal of Hydrometeorology*. Available from: http://dx.doi.org/10.1175/JHM-D-11-083.1 [Accessed March 2012].

Guildford, S.J. and Hecky, R.E., 2000. Total Nitrogen, Total Phosphorus, and Nutrient Limitation in Lakes and Oceans: Is There a Common Relationship? *Limnology and Oceanography*, 45 (6), 1213-1223.

Hanasaki, N., *et al.*, 2008. An integrated model for the assessment of global water resources. Part 1: Model description and input meteorological forcing. *Hydrology and Earth System Sciences*, 12, 1007–1025.

He, B., *et al.*, 2011. Assessment of global nitrogen pollution in rivers using an integrated biogeochemical modeling framework. *Water Research*, 45 (8), 2573-2586.

Hering, D., *et al.*, 2006. Assessment of European streams with diatoms, macrophytes, macroinvertebrates and fish: a comparative metric-based analysis of organism response to stress. *Freshwater Biology*, 51, 1757–1785.

Hoekstra A.Y., 2011. The Global Dimension of Water Governance: Why the River Basin Approach Is No Longer Sufficient and Why Cooperative Action at Global Level Is Needed. *Water*, 3 (1):21-46.

ICPDR, 2010. Available from: http://www.icpdr.org/icpdr-pages/industry.htm [Accessed Aug 2010].

IPCC, 2006. *IPCC Guidelines for National Greenhouse Gas Inventories. Volume 5: Waste.* Eggleston, S., Buendia, L., Miwa, K., Ngara, T., Tanabe, K. Eds. Hayama, Japan : IGES.

IVL *et al.*, 2007. *Hydrology and Water Resources Modelling, Work Package 4 Report.* TWINBAS-Twinning River Basins for Integrated water Resources Management, EU project No:505287.

Kämäri, J., *et al.*, 2008. Envisioning the future of water in Europe - the SCENES project. *E-WAter* [online], Article no. 2008/03. Available from: http://www.dwa.de/portale/ewa/ewa.nsf/home?readform&objectid=0AB6528C5177A8B7C12572B1004EF1C7&editor=no&&submenu=_1_6_2&&treeid=_1_6_2&

Krauze, P., Boyle, D.P., and Bäse, F., 2008. Comparison of different efficiency criteria for hydrological model assessment. *Advances in Geosciences*, 5, 89–97.

Król, K. and Sokół, A., 2006. Taming of nitrogen (in Polish). *Ekoprofit*, 6 (82), 23-31.

Lehner, B. and Döll, P., 2004. Development and validation of a global database of lakes, reservoirs and wetlands. *Journal of Hydrology*, 296 (1-4), 1-22.

Lehner, B., Verdin, K., and Jarvis, A., 2008. New global hydrography derived from spaceborne elevation data. *Eos, Transactions American Geophysical Union*, 89 (10), 93-94.

Lindström, G., *et al.*, 2010. Development and testing of the HYPE (Hydrological Predictions for the Environment) water quality model for different spatial scales. *Hydrology Research*, 41, 3–4.

Loomis, J., *et al.*, 2000. Measuring the total economic value of restoring ecosystem services in an impaired river basin: results from a contingent valuation survey. *Ecological Economics*, 33 (1), 103-117, ISSN 0921-8009, DOI: 10.1016/S0921-8009(99)00131-7.

Malve, O., *et al.*, accepted. Estimation of agricultural non-point load at the European scale. *Hydrological Processes*.

Meigh, J.R., McKenzie, A.A., and Sene, K.J., 1999. A Grid-Based Approach to Water Scarcity Estimates for Eastern and Southern Africa. *Water Resources Management*, 13, 85-115.

Meigh, J.R., Folwell, S., and Sullivan, C., 2005. Linking water resources and global change in West Africa: options for assessment. *In:* Wagener, T., Franks, S., Gupta, H.V., Bøgh, E., Bastidas, L., Nobre, C., and de Oliveira Galvão, C. Eds. *Regional hydrological impacts of Climate Change – Impact assessment and decision making*, Foz do Iguaçu, Brazil, April 2005. Wallingford, UK: IAHS Press, Publication No. 295, 297–303.

Michel, R.L., Pelmoter, A.L., and Palange, R.C., 1969. Operation and Maintenance of Municipal Waste Treatment Plants. *Water Pollution Control Federation*, 41 (3), 335-354.

Millenium Ecosystem Assessment, 2005. *Ecosystems and Human Well-Being.* Washington, DC: Island Press. Available from: http://maweb.org

Mitchell, G., 2001. *The Quality of Urban Stormwater in Britain and Europe: Database and Recommended Values for Strategic Planning Models.* University of Leeds (unpublished). Available from: http://www.geog.leeds.ac.uk/projects/nps/reports.htm [Accessed 3 October 2007].

Mitchell, T.D., *et al.*, 2004. *A comprehensive set of high-resolution grids of monthly climate for Europe and the globe: the observed record (1901–2000) and 16 scenarios (2001–2100).* Norwich, UK: Tyndall Centre for Climate Change Research, Technical Report Tyndall Working Paper 55.

Mitchell T.D. and Jones, P.D., 2005. An improved method of constructing a database of monthly climate observations and associated high resolution grids. *International Journal of Climatology*, 25, 693–712.

Moore, R. J., 2007. The PDM rainfall-runoff model. *Hydrology and Earth System Sciences*, 11 (1), 483-499.

Nelder, J.A. and Mead, R., 1965. A simplex method for function minimalization. *Computer Journal*, 7, 308-313.

Perry, J. and Venderklein, E., 1996. *Water quality: Management of a natural resource.* Oxford: Blackwell Science, ISBN 0-86542-469-1.

Pistocchi, A. and Pennington, D., 2006. European hydraulic geometries for continental SCALE environmental modelling. *Journal of Hydrology*, 329, 553–567.

Portmann, F.T., Siebert, S., and Döll, P., 2010. MIRCA2000 – Global monthly irrigated and rainfed crop areas around the year 2000: A new high-resolution data set for agricultural and hydrological modeling. *Global Biogeochemical Cycles*, 24, GB 1011, doi:10.1029/2008GB003435.

Rees, G. and Collins, D.N., 2004. *An assessment of the potential impacts of deglaciation on the water resources of the Himalaya.* London: DFID, Project R7980. Final technical report Volume 2.

Salvatore, M., *et al.*, 2005. *Mapping global urban and rural population distributions.* Rome: FAO, Environment and Natural Resources Working Paper 24.

SCENES, 2008. *Descriptions of the Regions and the Pilot Areas.* Kämäri. ed., Helsinki: Finnish Environment Institute, Report DIA2.1.

Seitzinger, S.P., *et al.*, 2005. Sources and delivery of carbon, nitrogen, and phosphorus to the coastal zone: An overview of Global Nutrient Export from Watersheds (NEWS) models and their application. *Global Biogeochemical Cycles*, 19, 1-11.

Siebert, S. and Döll, P., 2010. Quantifying blue and green virtual water contents in global crop production as well as potential production losses without irrigation. *Journal of Hydrology*, 384, 198-217.

Smith, R.A., Alexander, R.A., and Schwarz, G.E., 2003. Natural Background Concentrations of Nutrients in Streams and Rivers of the Conterminous United States. *Environmental Science and Technology*, 14 (37), 3039-3047.

Takata, K., Emori, S., and Watanabe, T., 2003. Development of the minimal advanced treatments of surface interaction and runoff. *Global And Planetary Change*, 38, 209–222.

Tate, E.L., Meigh, J.R., Prudhomme, C., and McCartney, M., 2000. *Drought assessment in Southern Africa using river flow data – Final report for Project R6573: Assessment of the Regional Impact of Drought in Africa (ARIDA)*. London: DFID, Project R6573, Report 00/4.

Tate, E.L. and Meigh, J.R., 2001. *Grid-based model of the Caspian Sea Basin: Phase II report.* Caspian Environment Program/EU-TACIS.

Tate, E., Dhlamini, S., and Meigh, J., 2002. *Southern Africa FRIEND phase 2. Water resources and climate change in Swaziland: A grid-based modelling approach.* Wallingford, UK: CEH.

USDA-SCS, 1993. Irrigation Water Requirements *in*: National Engineering Handbook, part 623. Washington, DC: USDA. Available from: ftp://ftp.wcc.nrcs.usda.gov/wntsc/waterMgt/irrigation/NEH15/ch2.pdf [Accessed 12 March 2012].

USGS, 1996. *GTOPO30.* Available from: http://edc.usgs.gov/products/elevation/gtopo30/gtopo30.html

USGS, 2001. *Global land cover characteristics data base version 2.0.* Available from: http://edcdaac.usgs.gov/glcc/globdoc2_0.html

Vogt, J., *et al.*, 2007. *A pan-European River and Catchment Database.* Luxembourg: European Commission - JRC, Report EUR 22920 EN.

Vörösmarty, C.J., *et al.*, 2010. Global threats to human water security and river biodiversity. *Nature*, 467, 555-561.

WHO / UNICEF *Joint Monitoring Programme (JMP) for Water Supply and Sanitation.* Available from: http://www.wssinfo.org/data-estimates/introduction/ [Accessed January 2010].

Williams, R., *et al.*, accepted. Assessment of current water pollution loads in Europe: Estimation of gridded loads for use in global water quality models. *Science of the Total Environment*.

Williams, R., Voß, A., Bärlund, I., and Keller, V., 2011 unpublished. *Joint manuscript on future of water quality in Europe according to SCENES scenarios.* European Commission, SCENES project, Deliverable 3.9.

WFD UK TAG, 2006. *UK Environmental standards and conditions (Phase 1).* UK Technical Advisory Group on the Water Framework Directive, Final report. Available from: www.wfduk.org

WFD UK TAG, 2007. *UK Environmental standards and conditions (Phase 2).* UK Technical Advisory Group on the Water Framework Directive, Final report. Available from: www.wfduk.org

Wint, W. and Robinson, T., 2007. *Gridded livestock of the world.* Rome: FAO.

Xu, C.Y. and Singh, V.P., 2004. Review on Regional Water Resources Assessment Models under Stationary and Changing Climate. *Water Resources Management*, 18, 591–612.

TABLES

Table 1 Input data for modelling water flows, their resolution, and source

Input data	Resolution	Source
Sub-grid elevation distribution[1]	30"	HydroSHEDS (Lehner *et al.* 2008), GTOPO (USGS, 1996)
Locations of irrigated crop types and the start and end of their growing season	5'	MIRCA2000 (Portman *et al.* 2008)
Crop characteristics and growth stage durations for 47 irrigated crop types	monthly, 5'	Allen (1998), Siebert and Doll (2010), MIRCA2000 (Portman *et al.* (2008)
Hydrography	n.a. (vector data)	CCM2.1 (Voght *et al.* 2007)
Soil texture	5'	HWSD (FAO *et al.* 2009)
Land cover	5'	GLCC (USGS 2001)
Climate parameters	10', monthly	CRU TS 1.2 (Mitchell *et al.* 2004)
Climate parameters	30', monthly	CRU TS 2.1 (Mitchell and Jones 2005)
Lake, reservoir and wetland parameters	5'	GLWD (Lehner and Döll 2004)
Fraction of water extracted from groundwater	country	Aquastat (FAO), Eurostat (European Commission 2010)
Urban, rural, and industrial water demand per capita	country	Eurostat (European Commission 2010)
Rural population[2]	5'	FAO (Salvatore *et al.* 2005)
Total population[2]	2.5'	GPW (Balk and Yetman 2004)
Cattle, sheep and goat population	0.05º	Wint and Robinson (2007)

[1]: Also used for calculating river depth during the simulation of pollutant transport
[2]: Also used for the modelling of pollutant loading from point sources and scattered settlements

Table 2 Input data for modelling agricultural pollutant loading to surface water bodies

Input data	Modelled pollutant	Source
Point source loading	TN, TP, BOD_5	This paper and Williams et al. (accepted)
Livestock units	TN, TP, BOD_5	Flörke and Alcamo (2004)
Runoff	TN, TP, BOD_5	GWAVA
Lake area	TN, TP	CCM2.1 (Voght *et al.* 2007)
Cropland area	TN	CLC2000 (2009), GLCC (2008)
slope	TP	Calculated from elevation data (Table 1)

Table 3 Critical levels used to indicate risk to biodiversity

Parameter	BOD_5 (mg L^{-1})	TP (mg L^{-1})	TN (mg L^{-1})
Statistic	90^{th} percentile	mean	mean
Critical level in running waters	4.5	0.22	5
Critical level in stagnant waters	-	0.022	1.5
Reference	UK TAG 2006, UK TAG, 2007	UK TAG 2006, UK TAG 2007	Król and Sokół 2006

Table C1 Model fit in 110 gauges having non-overlapping catchment areas. Fit is expressed using $\bar{e}_{abs}$ (%), $\Delta\mu$ (%), and Spearman's correlation coefficient *r* for model runs with and without calibrated parameters (indicated with 'Calibration' and 'Validation', respectively).

								Calibration			Validation		
Gauge	River	Country	Source	Gauge ID	Catchment area (Km^2)	First year	Last year	$\bar{e}_{abs}$	$\Delta\mu$	*r*	$\bar{e}_{abs}$	$\Delta\mu$	*r*
Ura e Dodes	Drin i Zi	AL	NCAR	9750	5390	1980	1984	16	-4	0.90	19	-8	0.89
Plovdiv	Maritza (Meric, Evros)	BG	NCAR	9762	7981	1980	1997	13	-1	0.78	19	-12	0.82
Elkhovo	Tundzha	BG	NCAR	80284	5550	1980	1997	26	0	0.87	43	36	0.83
Boboshevo	Struma (Strymon)	BG	NCAR	80283	-	1980	1997	12	-5	0.81	26	-22	0.81
Wittenberge	Elbe River	DE	GRDC	6340150	123532	1980	2000	16	-1	0.93	19	-8	0.91
Intschede	Weser	DE	GRDC	6337200	37720	1980	2000	18	-4	0.87	31	-28	0.84
Versen	Ems	DE	GRDC	6338100	8369	1980	2000	16	-1	0.94	22	-12	0.94
Narva (Hep)	Narva Jogi	EE	GRDC	6972350	56000	1980	1991	17	-2	0.88	20	-10	0.37
Tortosa	Ebro	ES	GRDC	6226800	84230	1996	1998	18	6	0.94	20	-8	0.94
Puente Pino	Duero	ES	GRDC	6212420	63160	1980	1991	15	-2	0.93	18	-9	0.93
Alcala Del Rio	Guadalquivir	ES	GRDC	6217100	46995	1980	1993	22	4	0.94	75	68	0.92
La Presa	Turia	ES	NCAR	80253	6294	1993	1998	50	49	0.94	168	166	0.32
Martorell	Llobregat	ES	GRDC	6227810	4561	1980	1989	12	-2	0.89	17	-12	0.91
Isohaara (Near The Mouth)	Kemijoki	FI	GRDC	6854700	50686	1980	2000	41	-37	-0.01	41	-37	-0.01
Anjala	Kymijoki	FI	GRDC	6855200	36275	1980	2000	14	-10	0.46	17	-15	0.67
Kalsinkosi	Kokemaenjoki	FI	GRDC	6854100	26025	1980	1992	16	-14	0.65	23	-20	0.74
Meriskoski (Near The Mouth)	Oulujoki	FI	GRDC	6854500	22841	1980	2000	54	-46	0.91	54	-46	0.91
Lake Inari Outlet	Paatsjoki	FI	GRDC	6830100	14575	1980	2000	60	-53	0.62	60	-53	0.62
Raasakka (Near The Mouth)	Iijoki	FI	GRDC	6854600	14191	1980	2000	52	-49	-0.02	52	-49	-0.02
Skatila (Lansorsund)	Kyronjoki	FI	GRDC	6854900	4833	1980	2000	34	-25	0.19	34	-29	0.37
Länkelä	Siika	FI	NCAR	33105	4395	1989	1990	25	-24	0.44	26	-24	0.30

Tolpankoski (Pyhankoski)	Pyhajoki	FI	GRDC	6854320	4283	1984	2000	44	-43	0.07	45	-40	0.21
Keppo	Lapuanjoki	FI	GRDC	6854200	3949	1980	2000	39	-36	0.14	40	-34	0.32
Haukipudas	Kiiminginjoki	FI	GRDC	6854400	3814	1980	2000	23	-9	0.22	23	-9	0.22
Simo	Simojoki	FI	GRDC	6854620	3109	1980	2000	48	-47	-0.02	48	-47	-0.02
Nikakoski (Near The Mouth)	Kalajoki	FI	GRDC	6854800	3065	1980	2000	21	-14	0.31	21	-14	0.31
Lohjanjarvi-Peltokoski	Karjaanjoki	FI	GRDC	6855500	1935	1980	2000	14	0	0.87	20	-9	0.88
Beaucaire	Rhone	FR	GRDC	6139100	95590	1980	1998	15	-5	0.90	18	-11	0.93
Kingston	Thames	GB	GRDC	6607650	9948	1980	2000	16	-1	0.94	20	-10	0.94
Colwick	Trent (N. England)	GB	GRDC	6605600	7486	1980	2000	15	-5	0.94	19	-10	0.94
Ballathie	Tay	GB	GRDC	6604610	4587	1980	2000	17	-2	0.94	22	-12	0.94
Norham	Tweed (Scotland)	GB	GRDC	6604750	4390	1980	2000	23	22	0.94	25	22	0.94
Bewdley	Severn (Central England)	GB	GRDC	6609500	4330	1980	2000	93	87	0.94	106	92	0.94
Boat O Brig	Spey (Scotland)	GB	GRDC	6604650	2861	1980	2000	147	133	0.93	149	134	0.93
Evesham	Avon (Central England)	GB	GRDC	6609400	2210	1980	2000	61	-54	0.93	61	-54	0.93
Bywell	Tyne	GB	GRDC	6605300	2176	1980	2000	45	44	0.94	45	44	0.94
Ilarion	Aliakmon	GR	GRDC	6261300	5005	1980	1987	14	2	0.93	20	-8	0.93
Temenos	Mesta (Nestos)	GR	GRDC	6264100	4393	1980	1989	12	-8	0.89	34	-29	0.88
Tisne stine	Cetina	HR	NCAR	80263	1456	1980	1998	140	132	0.90	140	132	0.90
Royal Oak	Barrow	IE	GRDC	6503351	2415	1980	2000	57	56	0.94	73	61	0.94
Slane Castle	Boyne	IE	GRDC	6503851	2408	1980	2000	46	42	0.94	49	46	0.94
Brownsbar	Nore	IE	GRDC	6503300	2388	1988	2000	14	-10	0.94	20	-8	0.94
Ballyduff	Blackwater (Munster)	IE	GRDC	6503500	2338	1991	2000	15	-8	0.94	20	-8	0.94
Clonmel	Suir	IE	GRDC	6503280	2173	1980	2000	16	-3	0.94	22	-12	0.94
Agan Naharayim	Jordan River	IL	GRDC	6594080	-	1989	1992	223	191	0.94	473	459	0.93
Thjorsartun	Thjorsa	IS	GRDC	6401120	7380	1980	2000	15	3	-0.32	17	-1	-0.49

Ferjubakki	Joekulsa A Fjoellum	IS	GRDC	6401701	7074	1980	1991	20	19	0.07	46	22	-0.45
Lagarfoss	Lagarfljot	IS	GRDC	6401800	2782	1980	2000	76	50	-0.28	89	49	-0.22
Kiljafoss	Hvita I Borgarfiroi	IS	GRDC	6401080	1669	1980	2000	16	-5	0.31	21	-11	0.36
Pontelagoscuro	Po	IT	GRDC	6348800	70091	1980	1997	15	-6	0.92	18	-11	0.92
Ripetta (Roma)	Tiber (Tevere)	IT	NCAR	9851	16545	1980	1997	16	-1	0.91	20	-17	0.91
San Giovanni alla Vena	Arno	IT	NCAR	80268	8186	1992	1997	14	-3	0.93	19	-18	0.91
Bronzolo (Branzoll)	Adige	IT	GRDC	6349200	6296	1980	1990	14	-13	0.62	17	-8	0.73
Santa Teresa	Pescara	IT	NCAR	80270	3125	1992	1997	17	6	0.18	18	3	0.56
San Samuele di Cafiero	Ofanto	IT	NCAR	33159	2716	1989	1994	34	1	0.92	56	49	0.91
Smalininkai	Nemunas - Neman	LT	GRDC	6974150	81200	1980	2000	17	-1	0.89	21	-11	0.86
Kudirkos Naumiestis	Sesupe - Sheshupe	LT	GRDC	6974201	3180	1997	2000	14	-1	0.91	17	-11	0.88
Kuldiga	Venta	LV	GRDC	6973010	8320	1980	1987	14	1	0.74	18	-2	0.80
Skopje	Vardar	MK	GRDC	6563200	4650	1980	1990	14	-7	0.92	23	-22	0.90
Lobith	Rhine River	NL	GRDC	6435060	160800	1980	2000	17	-2	0.91	20	-8	0.92
Lith	Meuse	NL	GRDC	6421100	29000	1980	1995	22	-1	0.91	23	3	0.91
Langnes	Glama	NO	GRDC	6731400	40540	1980	2000	33	-32	-0.12	33	-32	-0.12
Dovikfoss	Dramselv	NO	GRDC	6731310	16120	1980	2000	19	-19	0.33	19	-19	0.33
Polmak	Tana (No, Fi)	NO	GRDC	6730500	14165	1980	1999	39	-34	-0.29	39	-34	-0.29
Kista	Altaelva	NO	GRDC	6731920	6187	1980	2000	42	-39	-0.23	42	-39	-0.23
Bertnem	Namsen	NO	GRDC	6731555	5163	1980	2000	16	-8	0.21	16	-8	0.21
Heisel	Otra	NO	GRDC	6731260	3689	1980	2000	17	-9	0.88	17	-9	0.88
Lakfors	Vefsna	NO	GRDC	6731601	3650	1980	2000	30	-14	-0.01	40	-8	-0.09
Malangsfoss	Maalselv	NO	GRDC	6731907	3239	1980	2000	40	-38	-0.28	40	-38	-0.28
Neset	Neiden	NO	GRDC	6731330	2911	1980	2000	106	95	0.01	144	95	-0.24
Tczew	Vistula (Wisla)	PL	GRDC	6458010	194376	1980	1993	16	0	0.89	20	-9	0.85
Almourol	Tejo	PT	GRDC	6113050	67490	1988	1989	14	1	0.94	17	-13	0.94

Pulo Do Lobo	Guadiana	PT	GRDC	6116200	60883	1980	1989	31	27	0.94	42	35	0.94
Foz Do Mouro	Minho	PT	GRDC	6111100	15457	1986	1988	16	-4	0.93	19	-9	0.94
M.Da Gamitinha	Sado	PT	GRDC	6115500	2721	1980	1989	13	3	0.94	19	-1	0.94
Ceatal Izmail	Danube River	RO	GRDC	6742900	807000	1980	2000	16	-5	0.77	21	-9	0.80
Razdorskaya	Don	RU	GRDC	6978250	378000	1993	1995	16	-3	0.83	19	-12	0.11
Novosaratovka	Neva	RU	GRDC	6972430	281000	1980	1988	15	-3	-0.07	19	-8	-0.70
Tikhovsky	Kuban	RU	GRDC	6983350	48100	1996	1999	17	2	0.87	20	-12	0.73
Putkinskaya Ges	Kem (Trib. White Sea)	RU	GRDC	6972801	28700	1980	1988	21	-21	0.22	23	-22	-0.05
Matkozh	White Sea-Baltic Canal	RU	GRDC	6972135	26500	1980	1988	16	-7	0.36	19	-10	0.76
Knyazhegubskoye Ges	Kovda	RU	GRDC	6972860	25900	1980	1988	35	-34	-0.03	35	-34	-0.03
Serebryanskiy Ges 1	Voronya	RU	GRDC	6971401	8640	1980	2000	17	-12	-0.01	17	-12	-0.01
Varzuga	Varzuga	RU	GRDC	6971600	7940	1998	2000	61	37	0.18	63	37	-0.23
Oktiabrsky Railway,Km 1429	Kola	RU	GRDC	6971100	3780	1986	1992	45	-38	-0.35	45	-38	-0.35
At Efflux	Umba	RU	GRDC	6971151	2380	1980	1992	26	-23	-0.35	26	-23	-0.35
Pongoma	Pongoma	RU	GRDC	6972900	1220	1980	1988	69	63	0.12	69	63	0.12
Vaenersborg	Vaenern-Goeta	SE	GRDC	6229500	46885	1980	2000	17	1	0.91	21	-12	0.90
Kukkolankoski Oevre	Torneaelven	SE	GRDC	6233910	33930	1980	2000	28	-12	-0.44	28	-12	-0.44
Sollefteae Krv	Angermanaelven	SE	GRDC	6233650	30638	1980	2000	38	-34	0.37	38	-34	0.37
Aelvkarleby Krv	Dalaelven	SE	GRDC	6233201	28921	1980	2000	14	-11	0.45	17	-15	0.66
Bergeforsens Krv	Indalsaelven	SE	GRDC	6233401	25761	1980	2000	30	-26	0.37	30	-26	0.37
Bodens Krv (+ Vattenverk, Trangfors)	Luleaelven	SE	GRDC	6233750	24924	1998	2000	31	-29	-0.52	31	-29	-0.52
Raektfors	Kalixaelven	SE	GRDC	6233850	23103	1980	2000	52	-51	-0.59	52	-51	-0.59
Oevre Stockholm	Maelaren	SE	GRDC	6233410	22639	1980	2000	15	-7	0.79	21	-20	0.84
Ljusne Stroemmar Krv	Ljusnan	SE	GRDC	6233221	19817	1980	2000	15	-13	0.48	22	-19	0.49
Skallboele Krv	Ljungan	SE	GRDC	6233551	12088	1980	2000	39	-33	0.53	41	-36	0.78
Kvistforsens Krv	Skellefteaelven	SE	GRDC	6233690	11309	1980	2000	14	-13	0.40	17	-15	0.48

Sikfors Krv	Piteaelven	SE	GRDC	6233710	10816	1980	2000	36	-36	-0.42	36	-36	-0.42
Sorsele 2	Vindelaelven (Umeaelven)	SE	GRDC	6233680	6056	1980	2000	54	-45	-0.39	54	-45	-0.39
Angabaecks Krv	Lagan	SE	GRDC	6233170	5480	1980	2000	17	1	0.94	22	-7	0.93
Emsfors Bruk	Eman	SE	GRDC	6233360	4446	1980	2000	14	-2	0.92	19	-8	0.91
Niemisel	Raneaelven	SE	GRDC	6233780	3781	1980	2000	43	-41	-0.33	44	-42	-0.28
Torebro Krv (Powerstation)	Helge A	SE	GRDC	6233250	3665	1980	2000	26	-23	0.93	26	-23	0.93
Torrboele	Oereaelven	SE	GRDC	6233720	2860	1980	2000	44	-38	-0.12	44	-38	-0.12
Asbro 3	Viskan	SE	GRDC	6233100	2160	1980	2000	14	-12	0.93	20	-20	0.93
Hallbosjoen	Nykoepingsaen	SE	GRDC	6233440	1992	1980	2000	36	-32	0.87	40	-36	0.76
Kakhovskoye Vodokhranilishche Ges	Dnepr	UA	GRDC	6980802	482000	1980	1988	16	6	0.89	34	33	0.81
Redbrook	Wye	UK	NCAR	80335	4010	1991	1999	60	59	0.94	62	60	0.94
Offord	Bedford Ouse	UK	NCAR	80302	2570	1980	1996	23	22	0.94	57	53	0.93

FIGURES

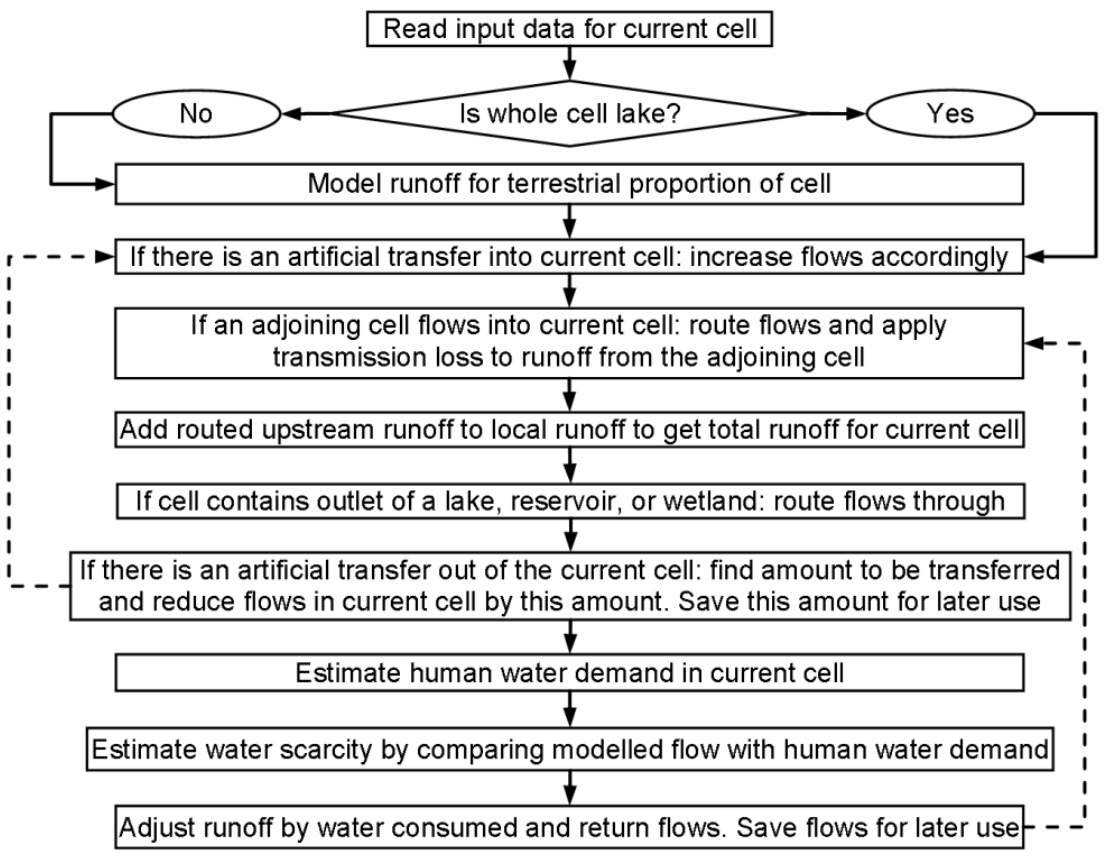

Fig. 1 Structure of GWAVA illustrated for a single grid cell (based on Meigh *et al.* 1999). Transfer of data to and from different cells is indicated with dashed arrows.

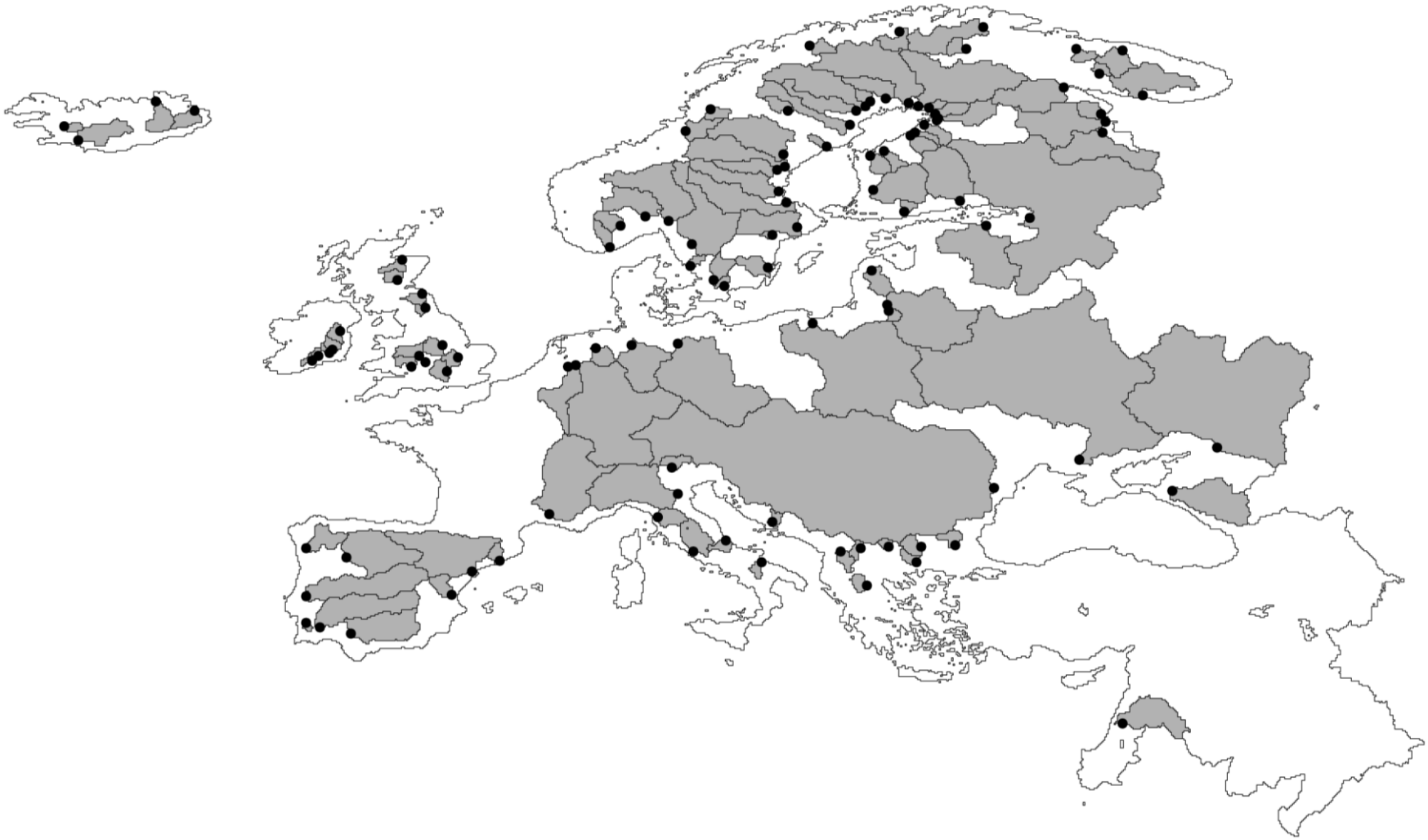

Fig. 2a Locations of gauging stations used for validation of modelled water quantity. Gauge locations are shown with black dots and their upstream areas are shown in grey.

Fig. 2b Locations of gauging stations used for validation of modelled water quality. Gauge locations are shown with black dots and their upstream areas are shown in grey.

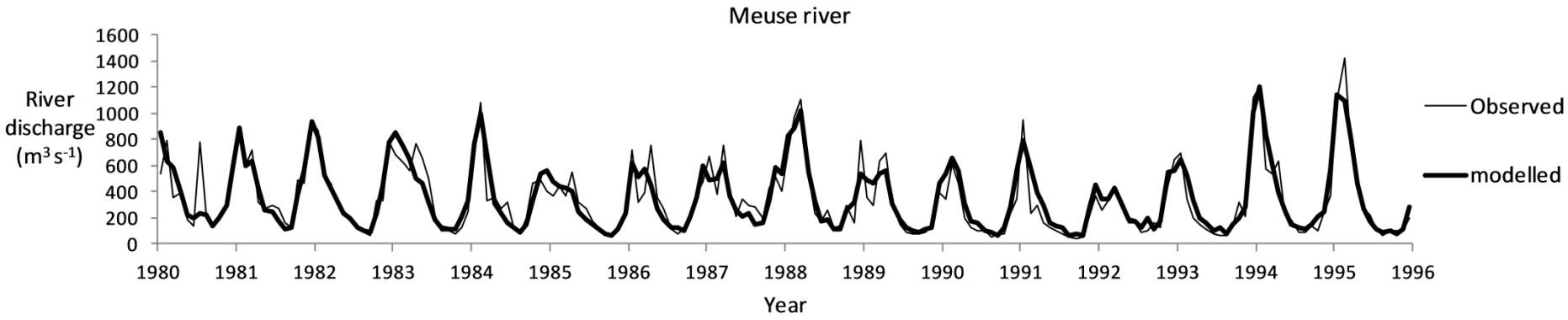

Fig. 3 Comparison of modelled and observed monthly discharge in the Meuse river at GRDC station Lith.

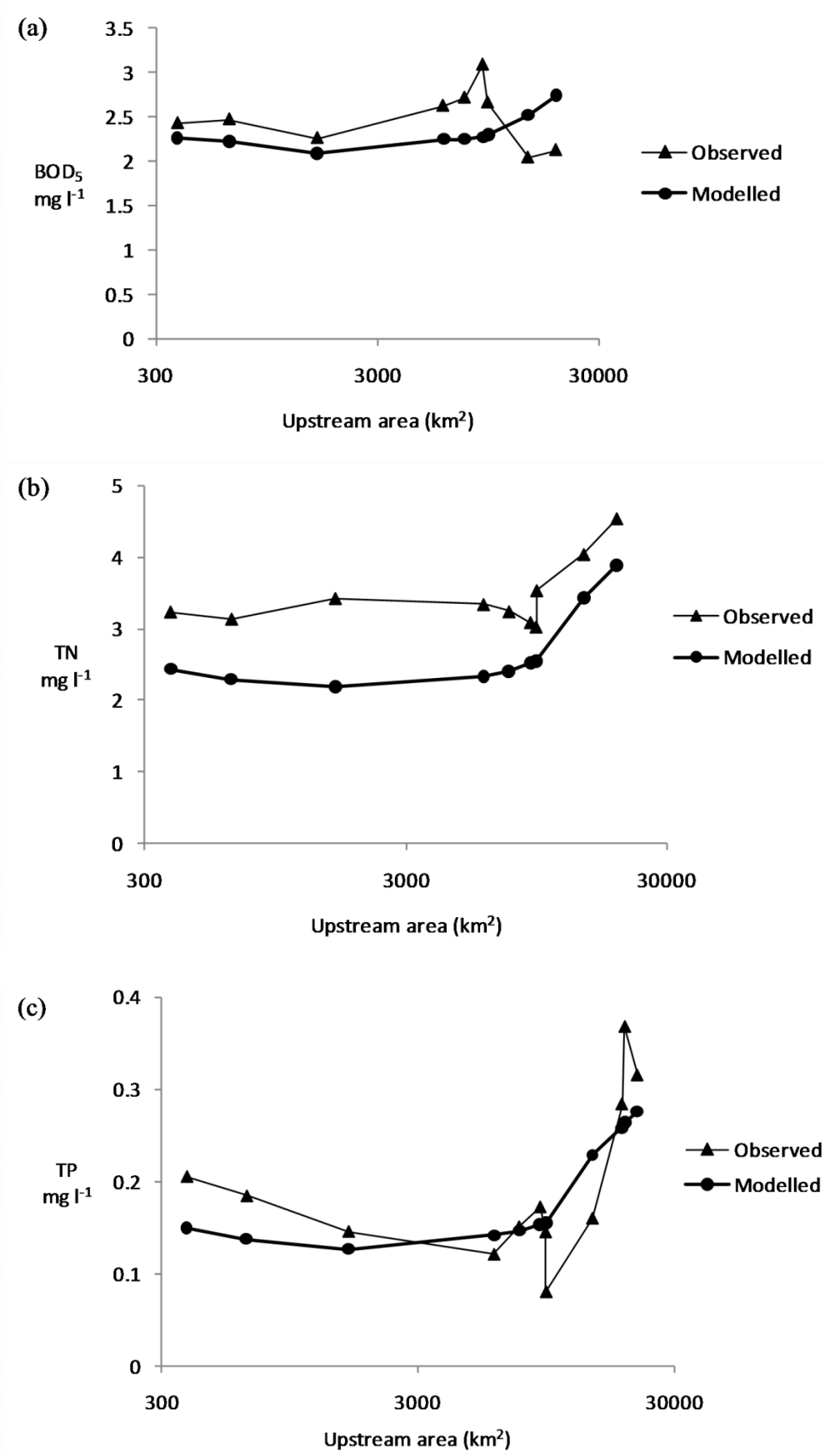

Fig. 4 Modelled and observed annual average pollutant levels along the Meuse river around the year 1999. a: BOD_5; b: TN; c: TP.

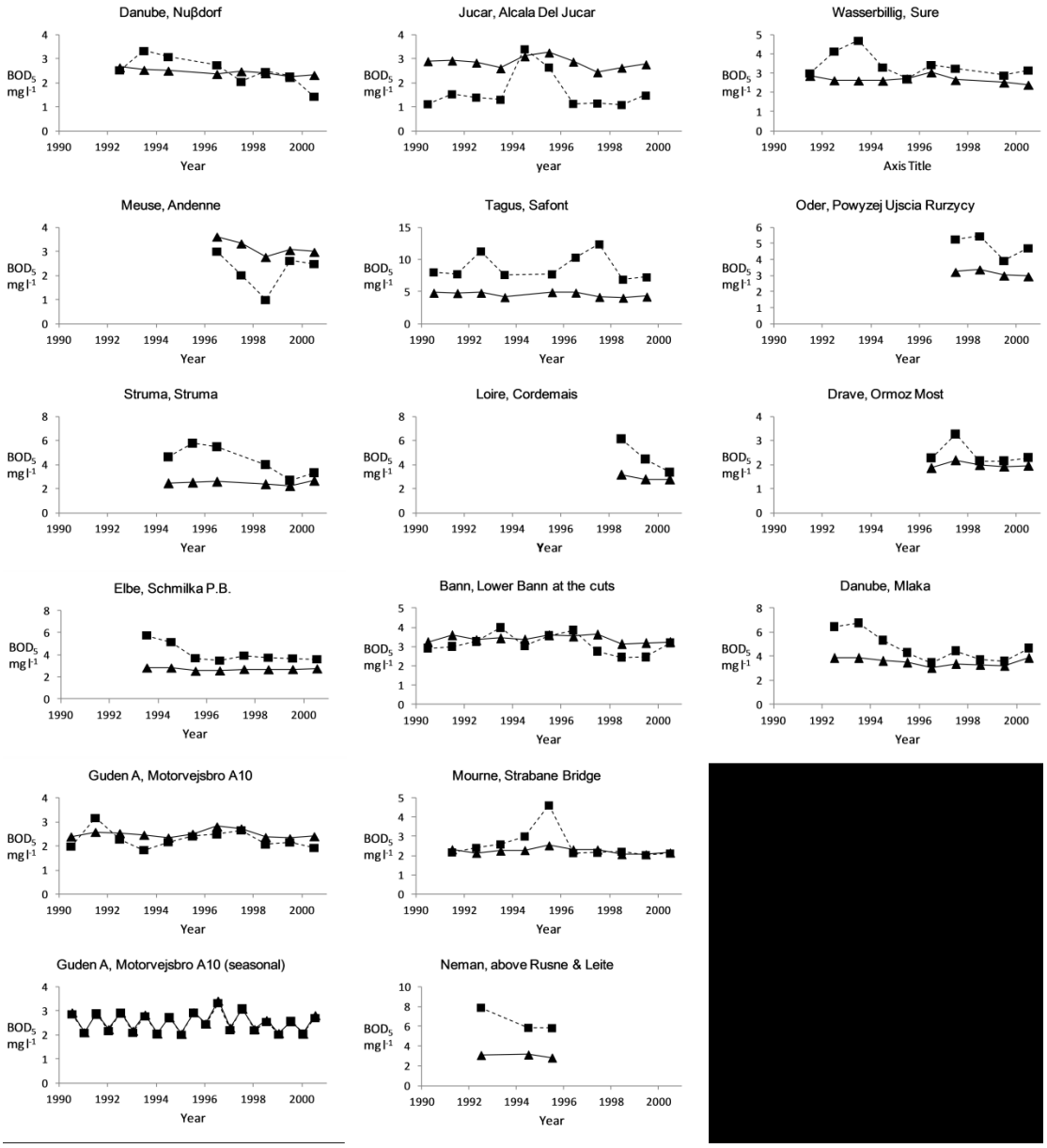

Fig. 5 Time series of modelled and observed BOD_5 levels at the selected river water quality measurement stations. Annual average BOD_5 levels are shown, unless the time-series header indicates that seasonal averages are shown. Triangles indicate modelled values and squares indicate measured values. Both modelled and measured values are aggregated over the same season or year.

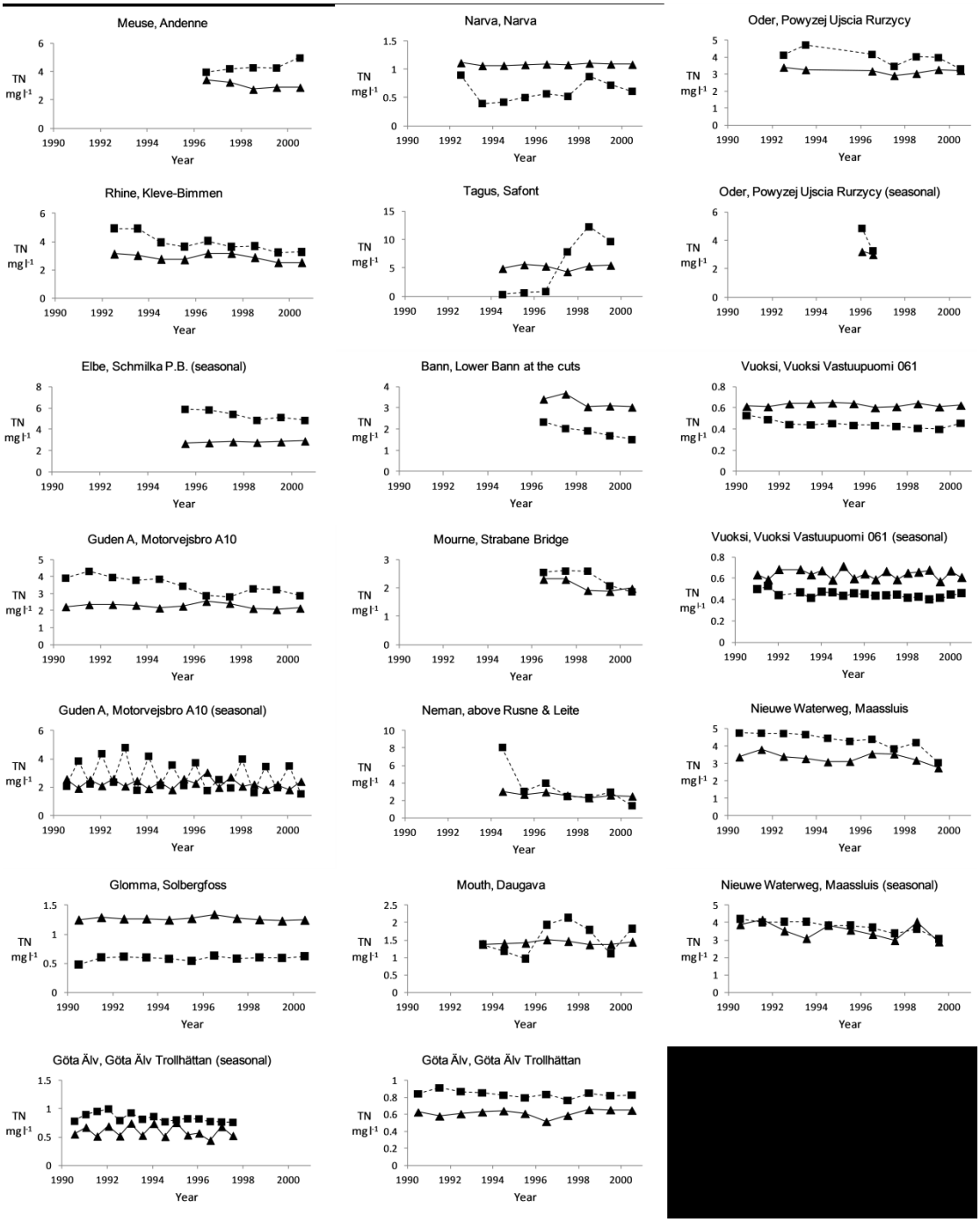

Fig. 6 Time series of modelled and observed TN concentrations at the selected river water quality measurement stations. Annual average TN concentrations are shown, unless the time-series header indicates that seasonal averages are shown. Triangles indicate modelled values and squares indicate measured values. Both modelled and measured values are aggregated over the same season or year.

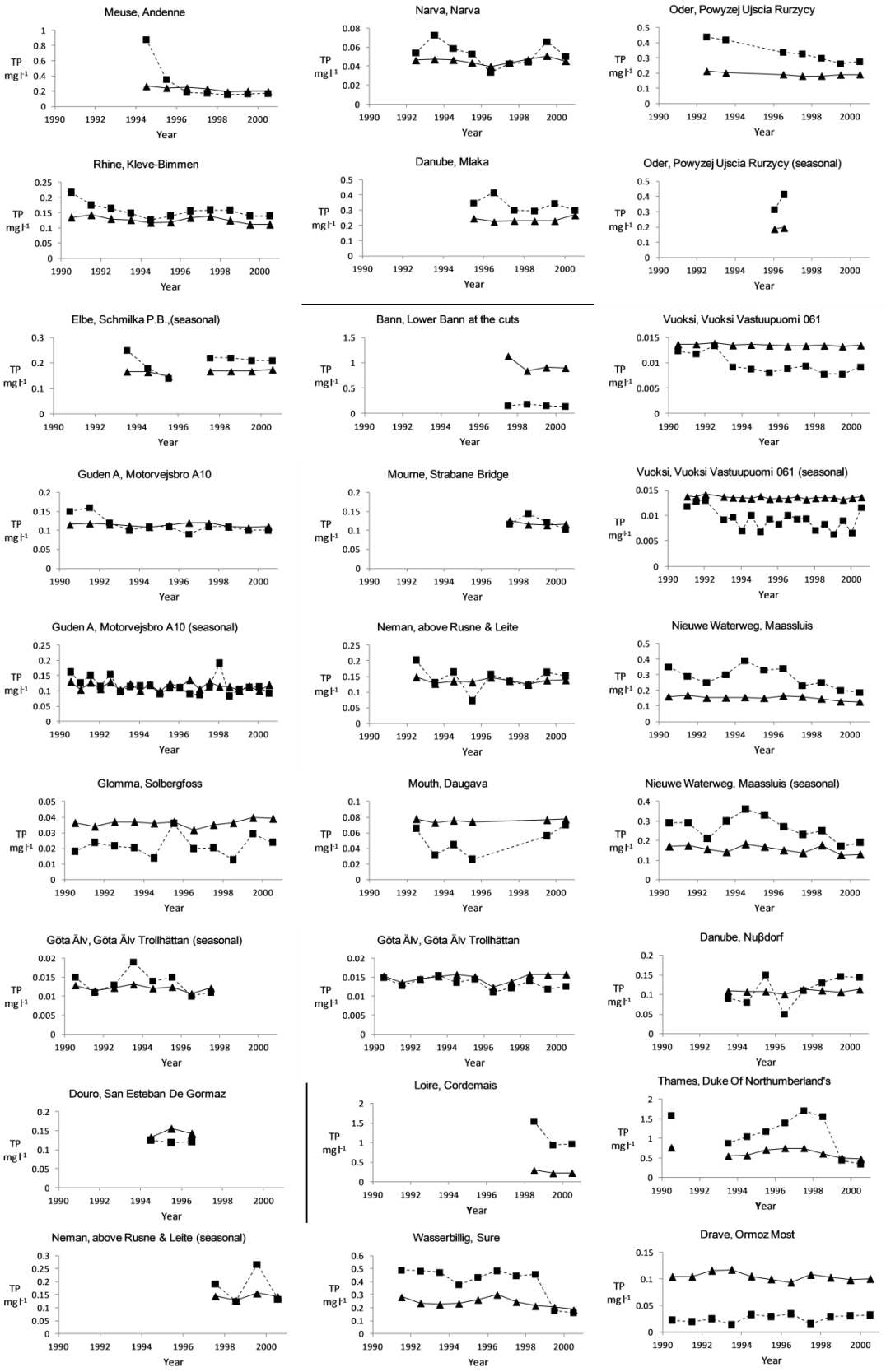

Fig. 7 Time series of modelled and observed TP concentrations at the selected river water quality measurement stations. Annual average TP concentrations are shown, unless the time-series header indicates that seasonal averages are shown. Triangles indicate modelled values and squares indicate measured values. Both modelled and measured values are aggregated over the same season or year.

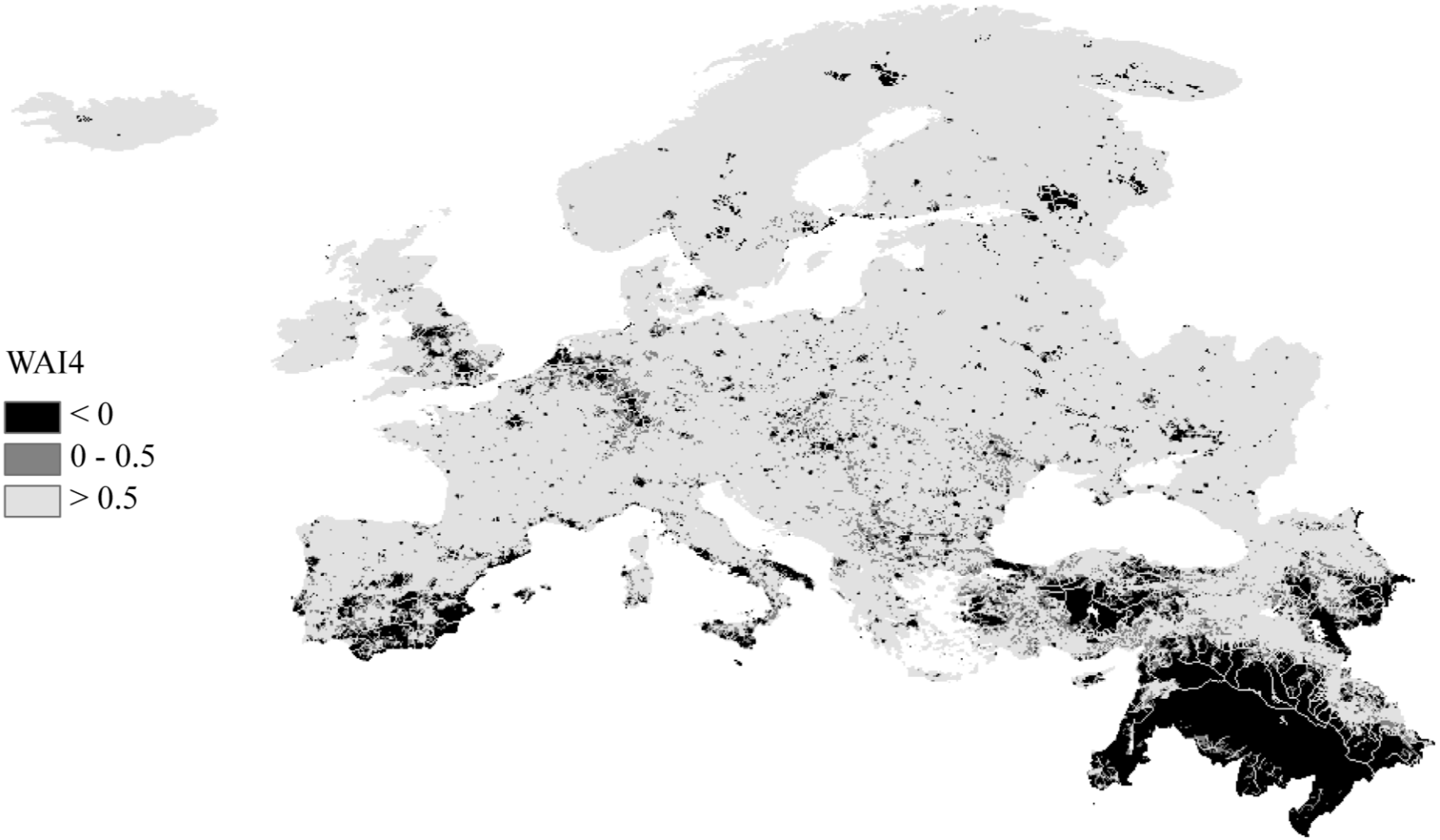

Fig. 8 Modelled human water security from 1990 to 2000 across Europe indicated by WAI4. WAI4 has a higher value if the available water quantity better fulfils the human demand for water.

Fig. 9a Modelled 90th percentile BOD_5 level in surface waters aggregated over the period 1990-2000. Concentrations are only shown where surface water was present in all modelled months. Mapped pollution levels correspond with the critical levels used to indicate risk to biodiversity (Table 3).

Fig. 9b Modelled mean TN concentration in surface waters aggregated over the period 1990-2000. Concentrations are only shown where surface water was present in all modelled months. Mapped pollution levels correspond with the critical levels used to indicate risk to biodiversity (Table 3).

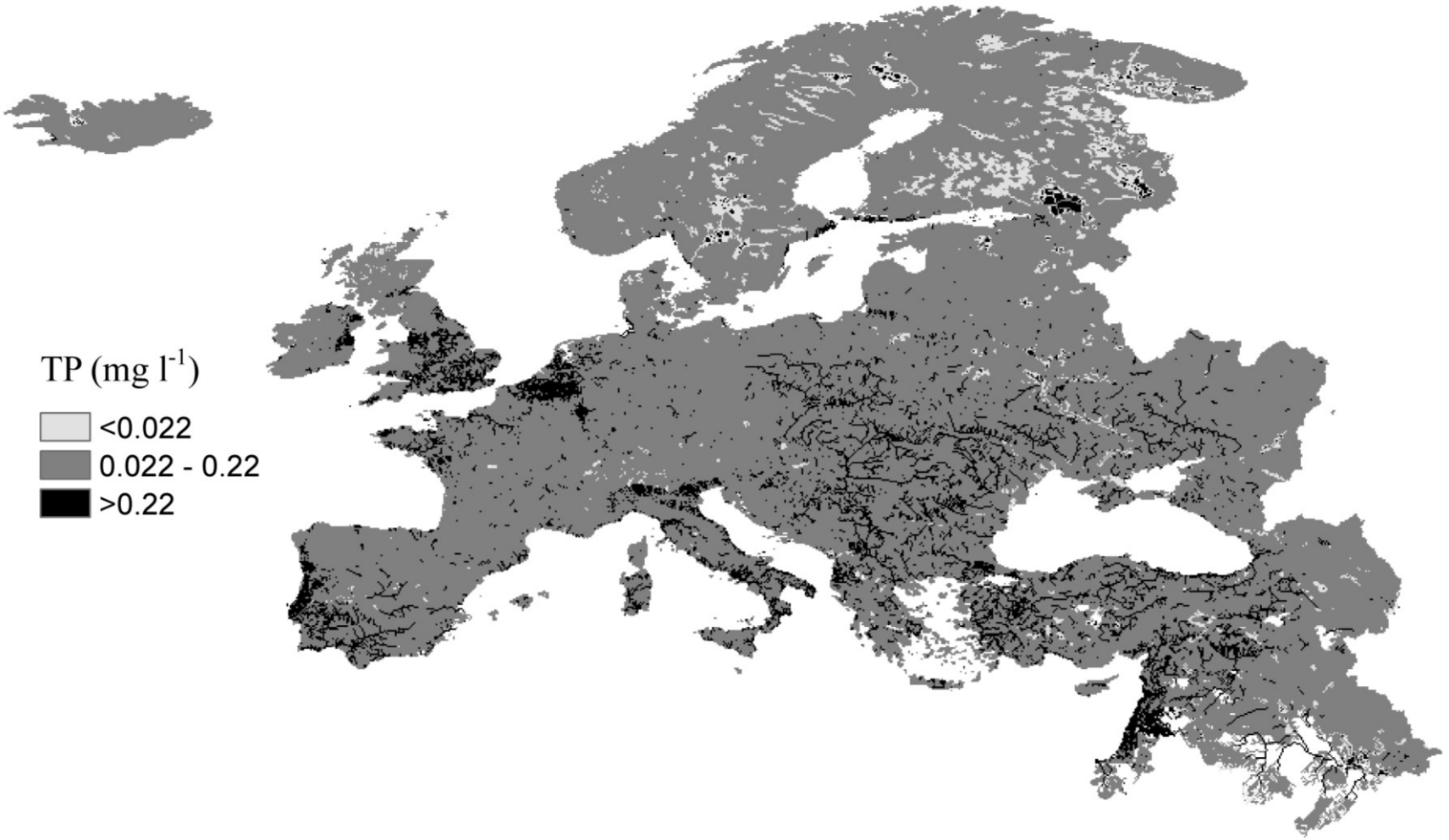

Fig. 9c Modelled mean TP concentration in surface waters aggregated over the period 1990-2000. Concentrations are only shown where surface water was present in all modelled months. Mapped pollution levels correspond with the critical levels used to indicate risk to biodiversity (Table 3).

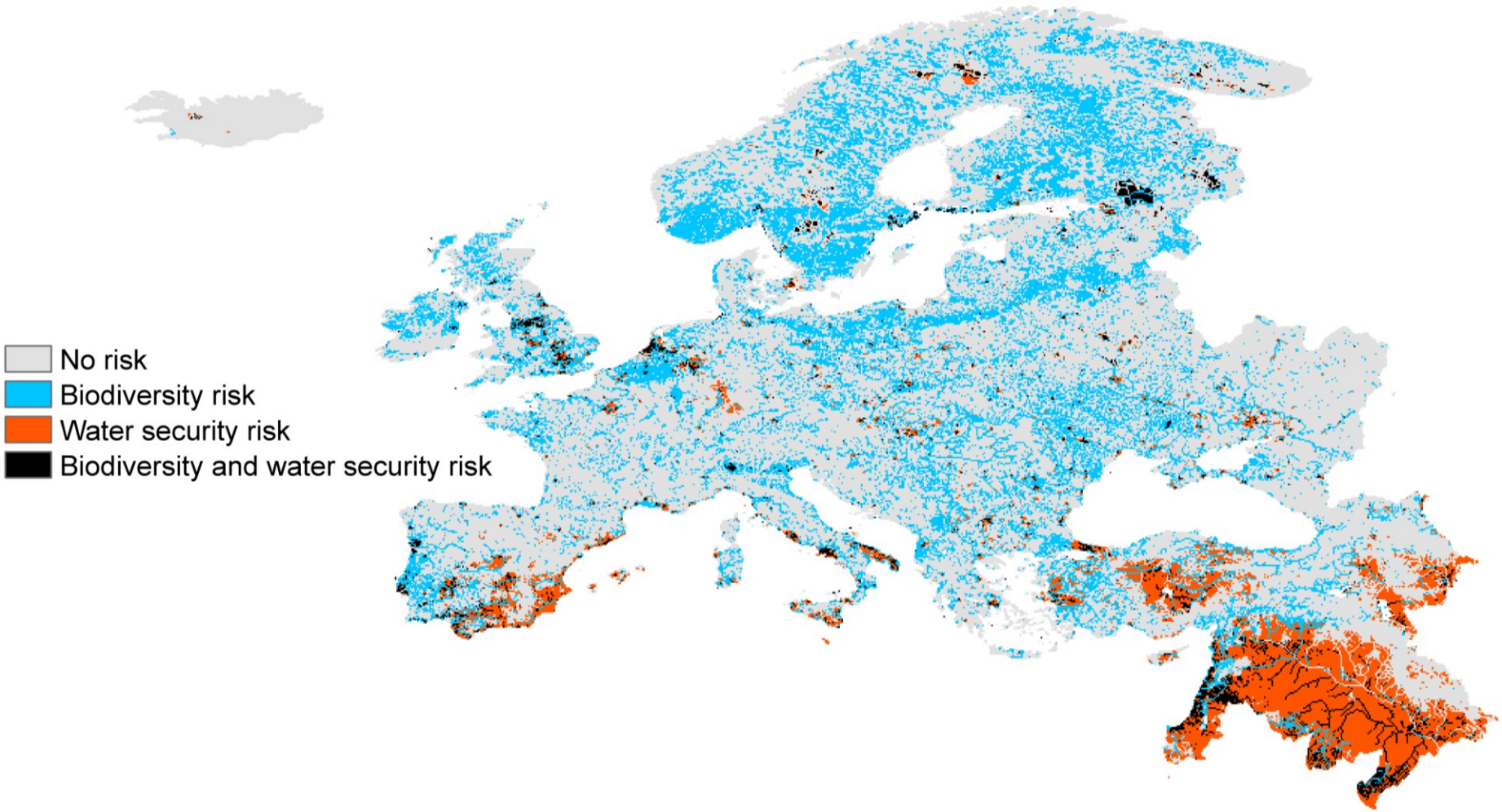

Fig. 10 Locations where the model indicates risk for human water security and aquatic biodiversity. Risk for aquatic biodiversity is indicated if the TP, TN, or BOD_5 level is above the standard given in Table 3. Risk for human water security is indicated if WAI4 (equation (12)) is negative. Risk for aquatic biodiversity is only shown where surface water was present in all modelled months.